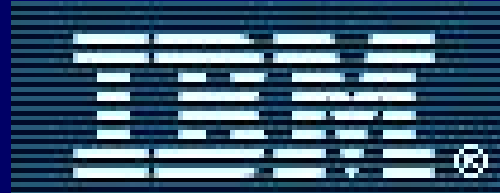

Superconducting Qubits

David DiVincenzo, IBM

Ann Arbor Summer School, 6/2008





Scanned at the American
Institute of Physics

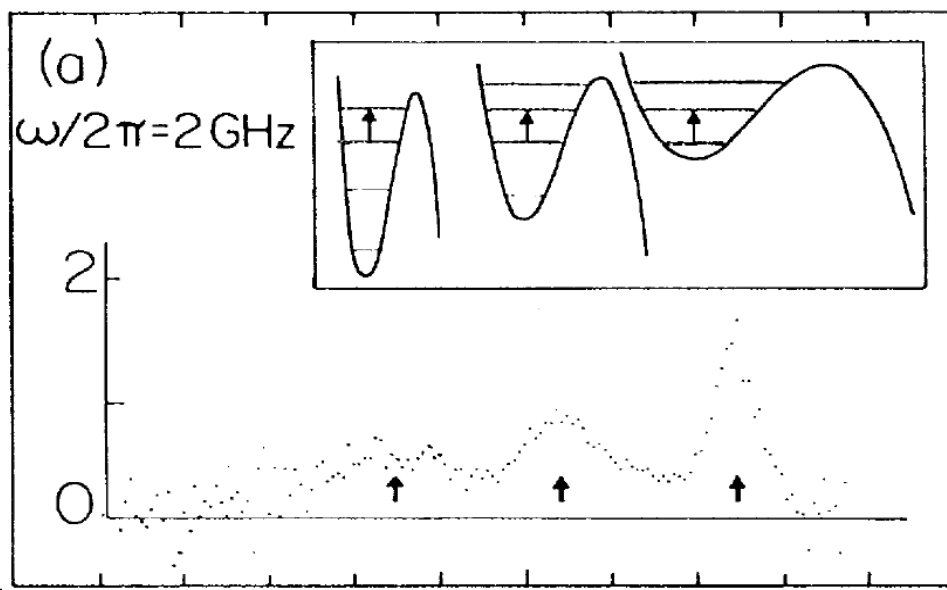
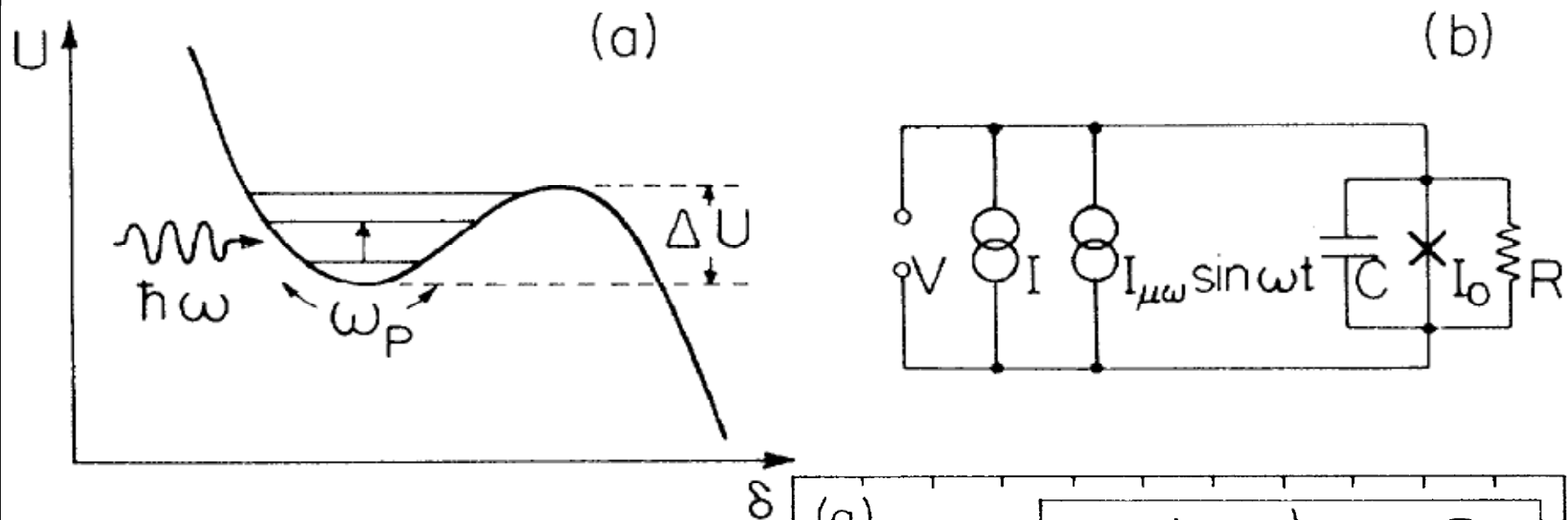


Scanned at the American
Institute of Physics

Description: L-R: A.J. Rutgers; Hendrik Casimir in an automobile they bought for \$50.00 to drive from Ann Arbor, Michigan to New York City where they abandoned it. (photo: S. Goudsmit.)

Energy-Level Quantization in the Zero-Voltage State of a Current-Biased Josephson Junction

John M. Martinis, Michel H. Devoret,^(a) and John Clarke



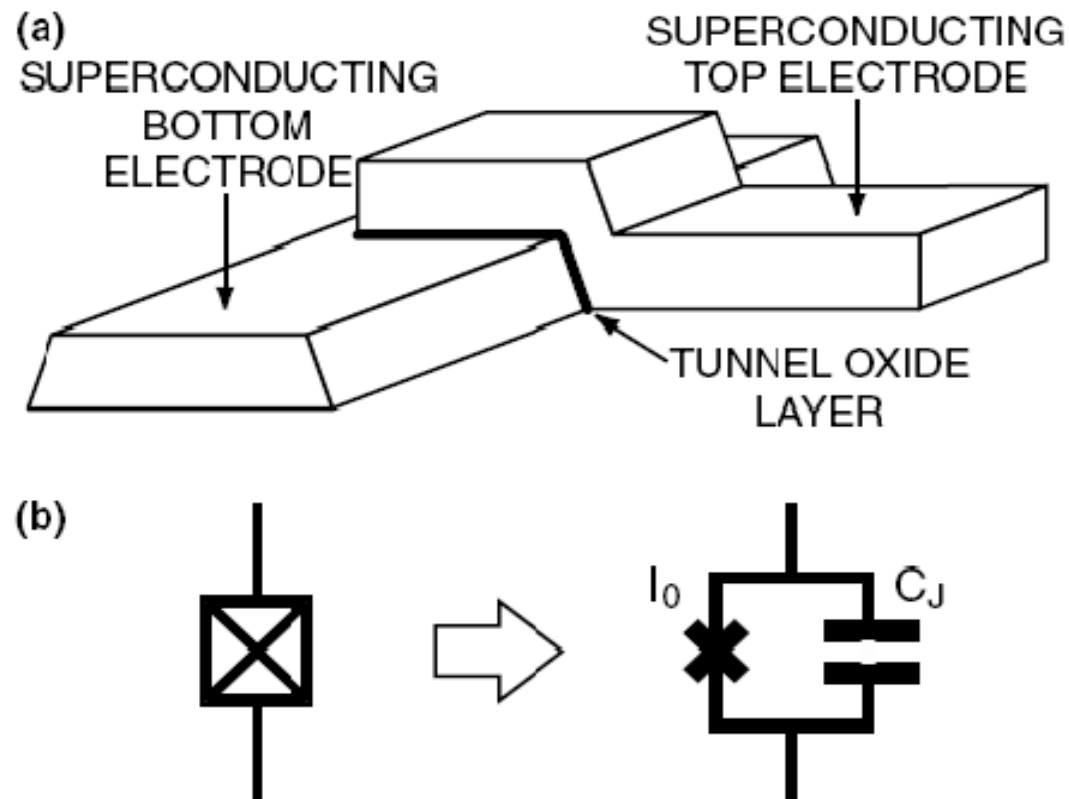


Fig. 1. (a) Josephson tunnel junction made with two superconducting thin films; (b) Schematic representation of a Josephson tunnel junction. The irreducible Josephson element is represented by a cross.

The discovery of tunnelling supercurrents*

B. D. Josephson

Reviews of Modern Physics, Vol. 46, No. 2, April 1974

Cavendish Laboratory, Cambridge, England

ascribed to the tunnelling process.

Anderson and Rowell (1963) that such supercurrents could be definitely

supercurrent is clearly visible. It was not until the experiments of

evaporated-film superconductors (Smith et al., 1961). A zero-voltage

Fig. 3 The first published observation of tunnelling between two

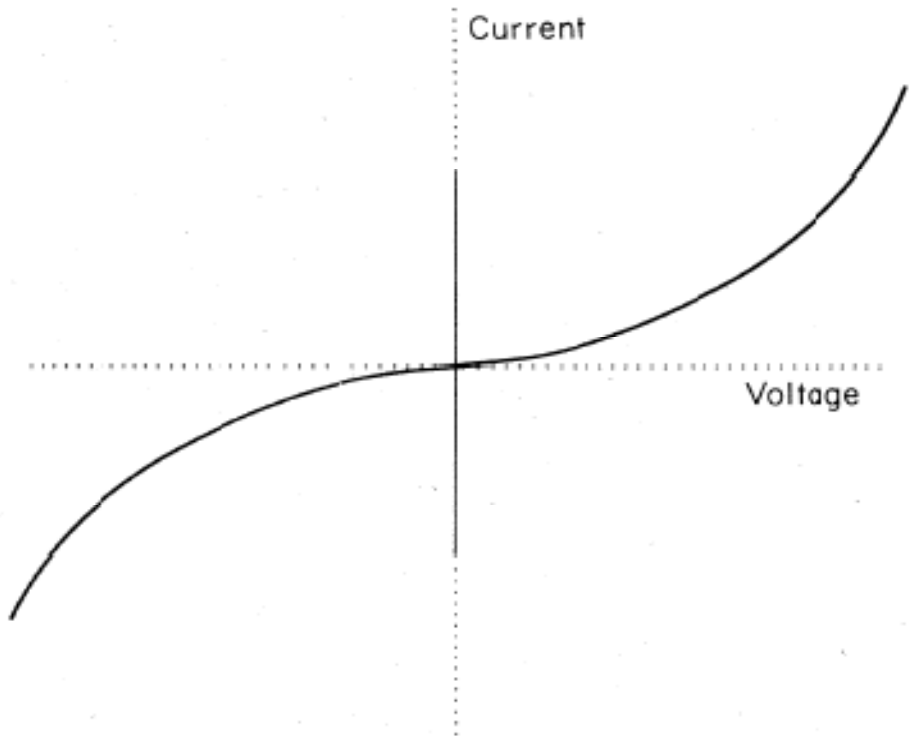
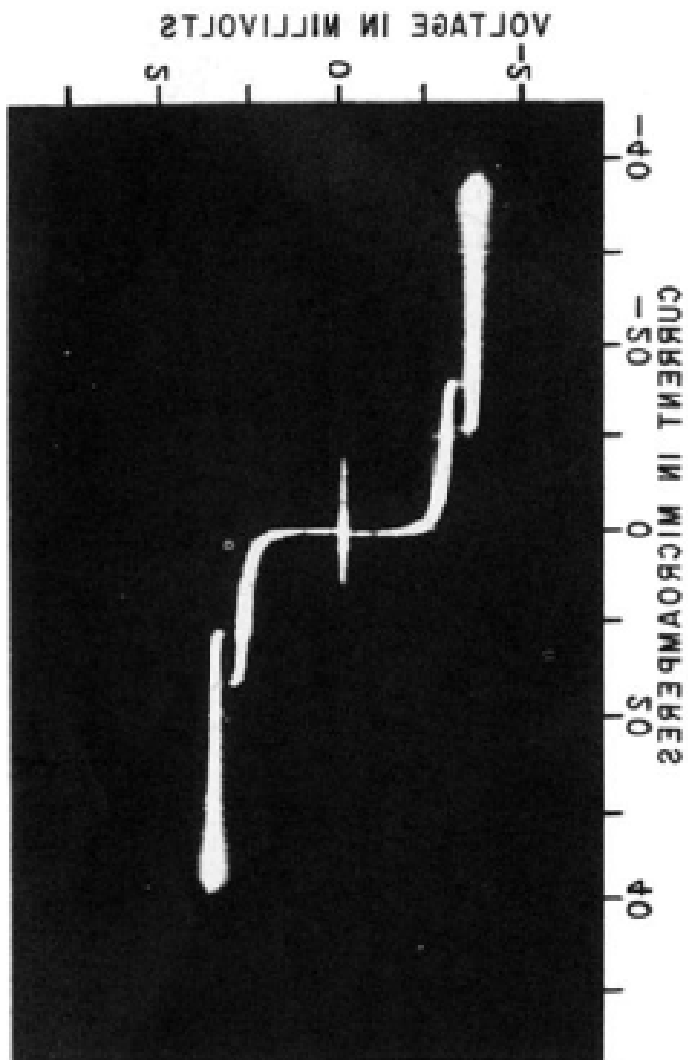


FIG. 2. Predicted two-part current-voltage characteristic of a superconducting tunnel junction.

QUANTUM FLUCTUATIONS IN ELECTRICAL CIRCUITS

Michel H. Devoret

S. Reynaud, E. Giacobino and J. Zinn-Justin, eds.

Les Houches, Session LXIII, 1995

Fluctuations Quantiques

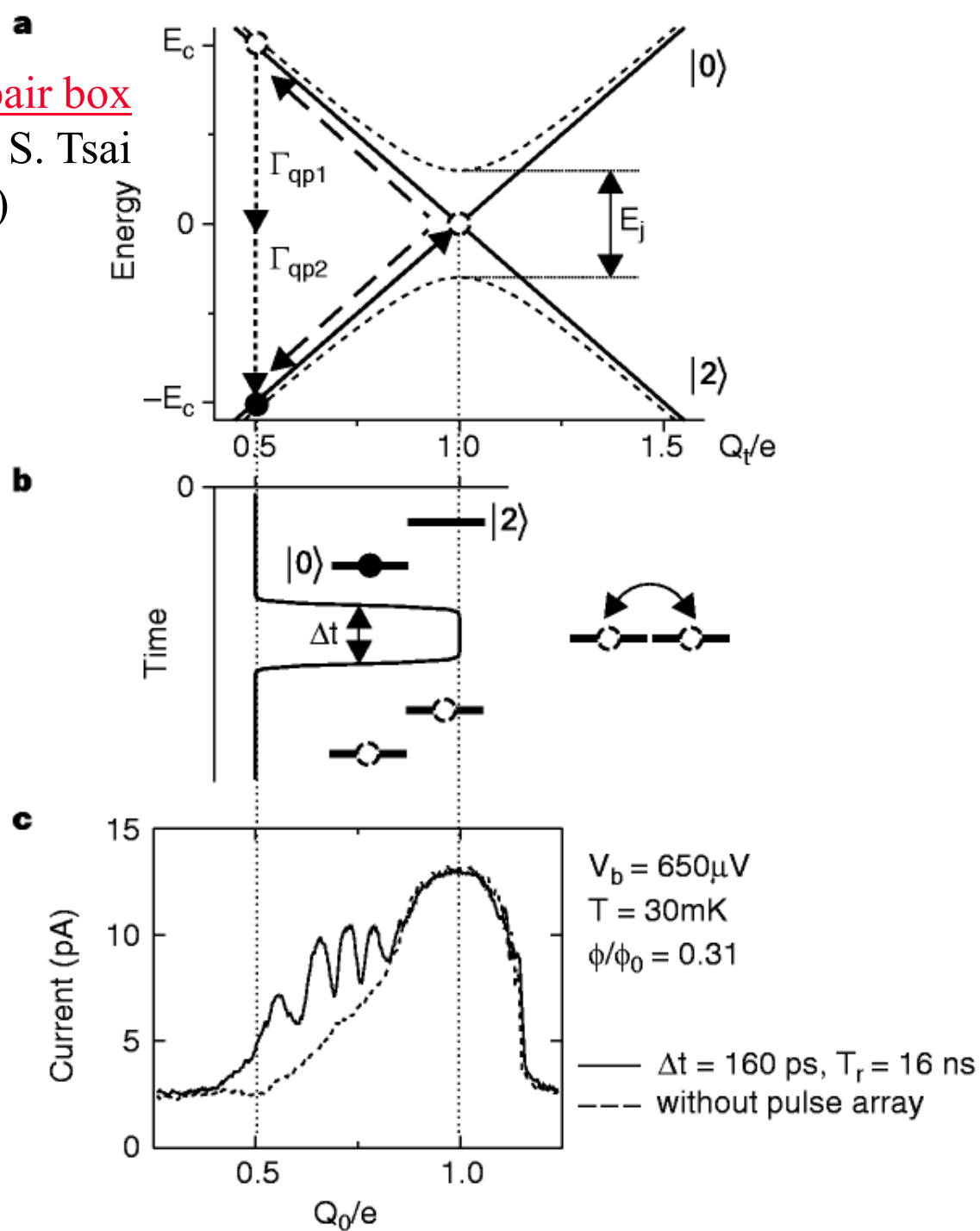
Quantum Fluctuations

© 1997 Elsevier Science B.V. All rights reserved

Josephson junctions are so well coupled to their electromagnetic environment that dissipation cannot be treated as a perturbation. In fact, dissipation combines with the non-linearity of tunnel elements to produce qualitatively new quantum effects which are not encountered for example in the almost dissipation-free quantum systems studied in atomic physics. The most spectacular new quantum feature is the localization of position-like degrees of freedom when dissipation exceeds a certain threshold set by the quantum of resistance $h/(2e)^2 \simeq 6.4 \text{ k}\Omega$ [8–10].

Coherent control of macroscopic quantum states in a single-Cooper-pair box

Y. Nakamura, Yu. A. Pashkin and J. S. Tsai
Nature 398, 786-788(29 April 1999)

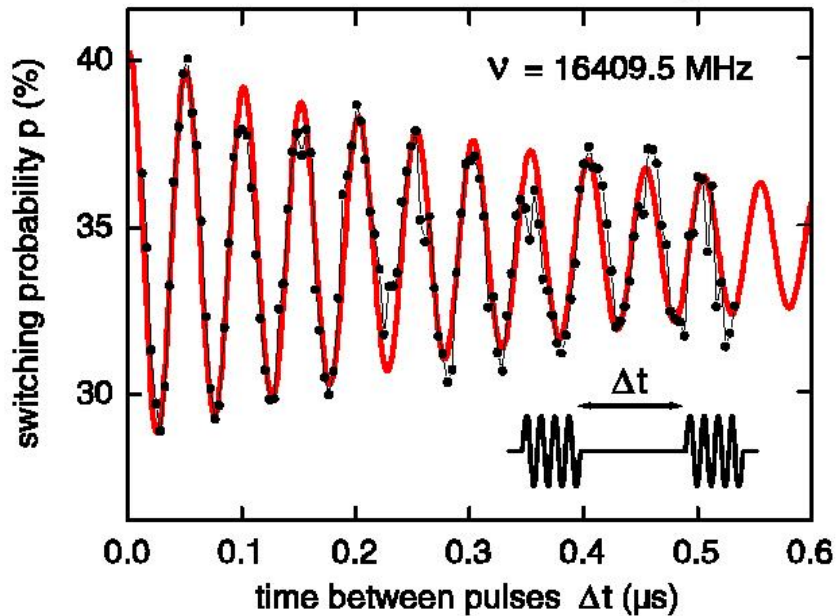


Saclay Josephson junction qubit

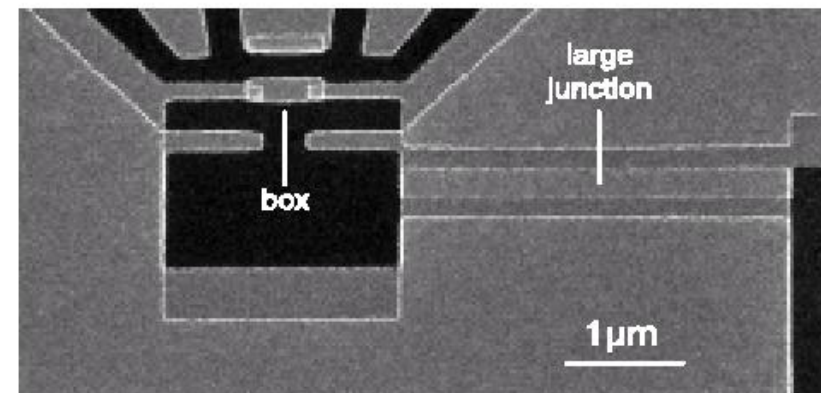
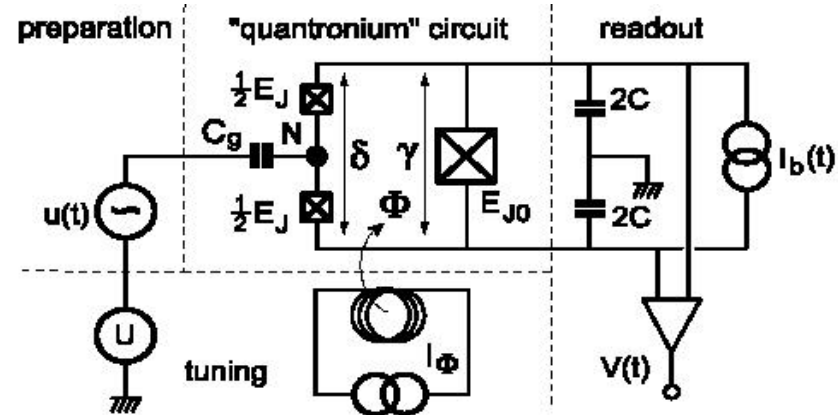
Manipulating the quantum state of an electrical circuit

Science 296, 886 (2002)

D. Vion, A. Aassime, A. Cottet, P. Joyez, H. Pothier, C. Urbina, D. Esteve and M.H. Devoret

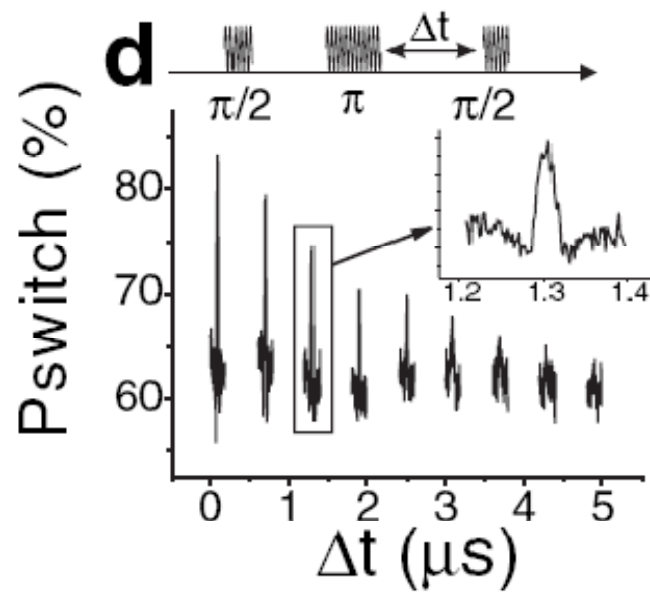
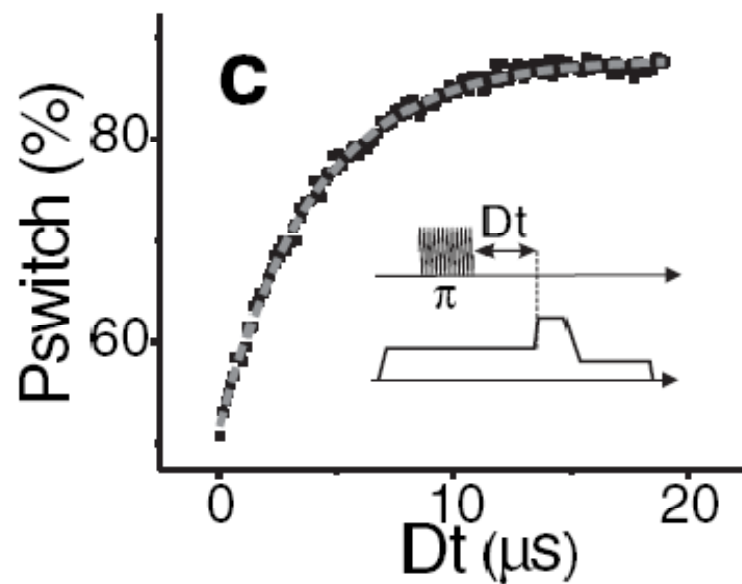
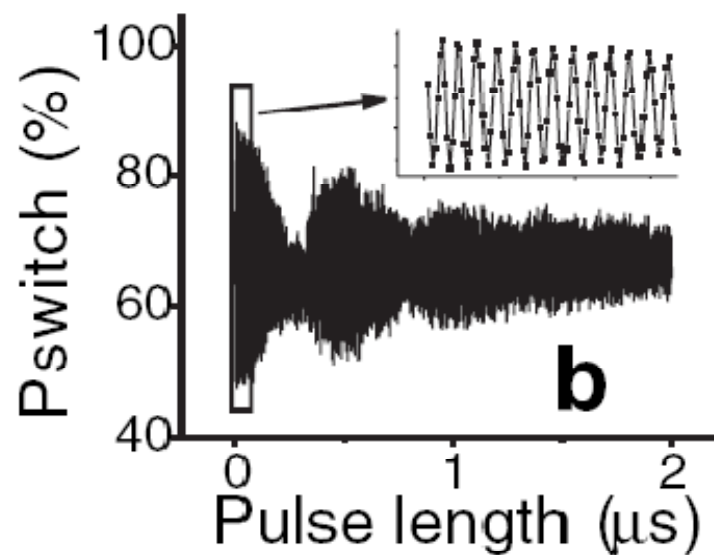
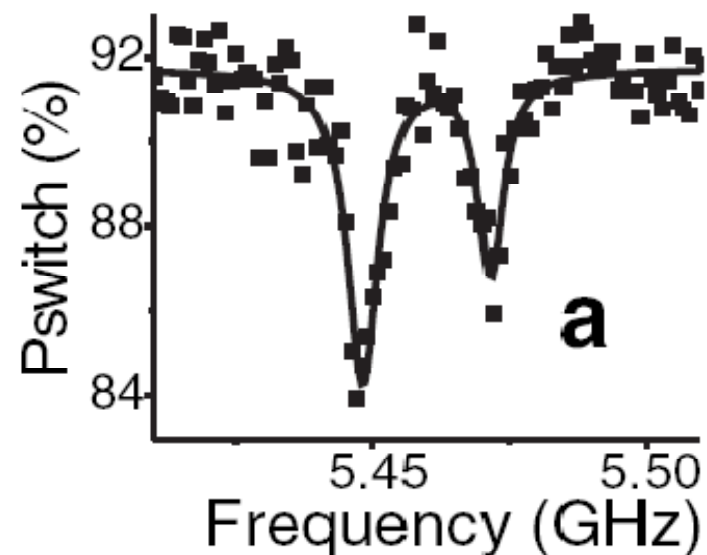


Oscillations show rotation of qubit at constant rate, with noise.

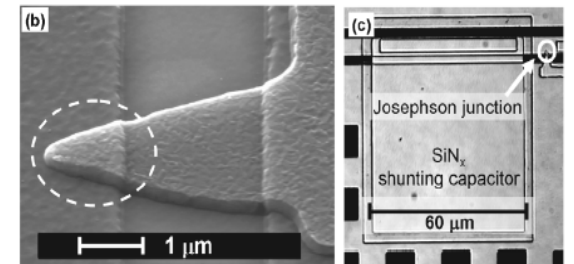
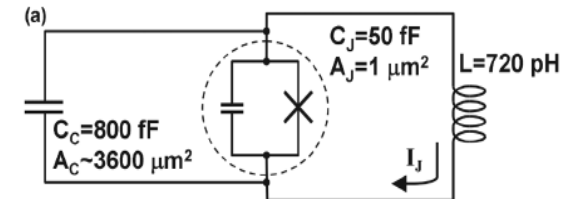
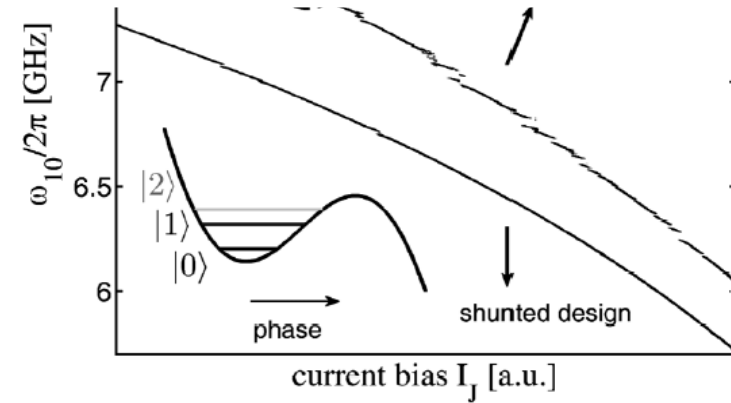
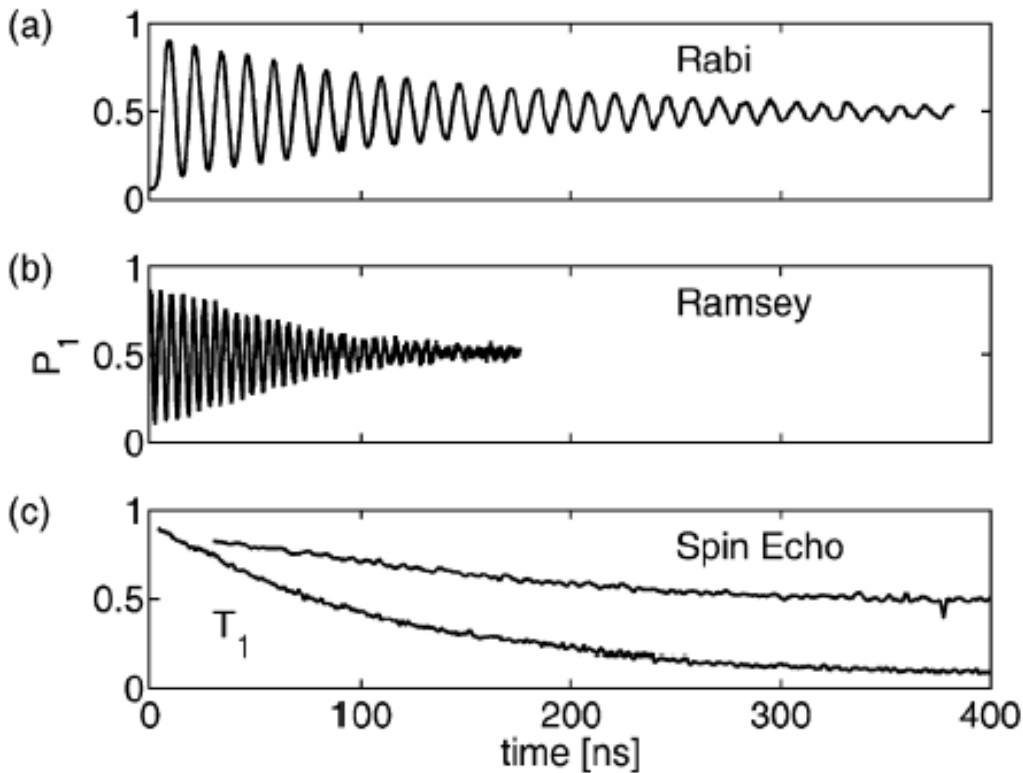


Dephasing of a Superconducting Qubit Induced by Photon Noise

P. Bertet,¹ I. Chiorescu,^{1,*} G. Burkard,^{2,3} K. Semba,^{1,4} C.J.P.M. Harmans,¹ D.P. DiVincenzo,² and J.E. Mooij¹



UCSB Josephson junction qubit (“phase”)



PRL 97, 050502 (2006)

PHYSICAL REVIEW LETTERS

week ending
4 AUGUST 2006

State Tomography of Capacitively Shunted Phase Qubits with High Fidelity

Matthias Steffen, M. Ansmann, R. McDermott, N. Katz, Radoslaw C. Bialczak, Erik Lucero, Matthew Neeley, E.M. Weig, A.N. Cleland, and John M. Martinis*

Department of Physics and California Nanosystems Institute, University of California, Santa Barbara, California 93106, USA

Temperature dependence of coherent oscillations in Josephson phase qubits

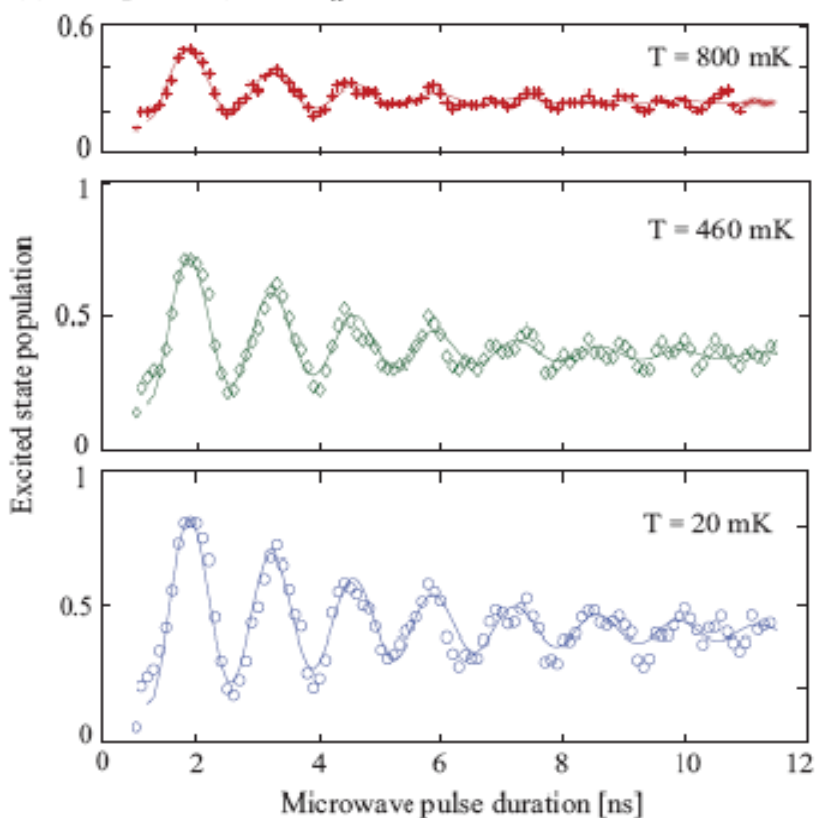
J. Lisenfeld¹, A. Lukashenko¹, M. Ansmann², J. M. Martinis², and A. V. Ustinov^{1*}

¹ *Physikalisches Institut III, Universität Erlangen-Nürnberg, D-91058 Erlangen, Germany*

² *Department of Physics and California Nanosystems Institute, University of California, Santa Barbara, California 93106, USA*

(Dated: February 1, 2008)

(a) sample #1 (Nb SiO₂)



(b) sample #2 (Al SiN_x)

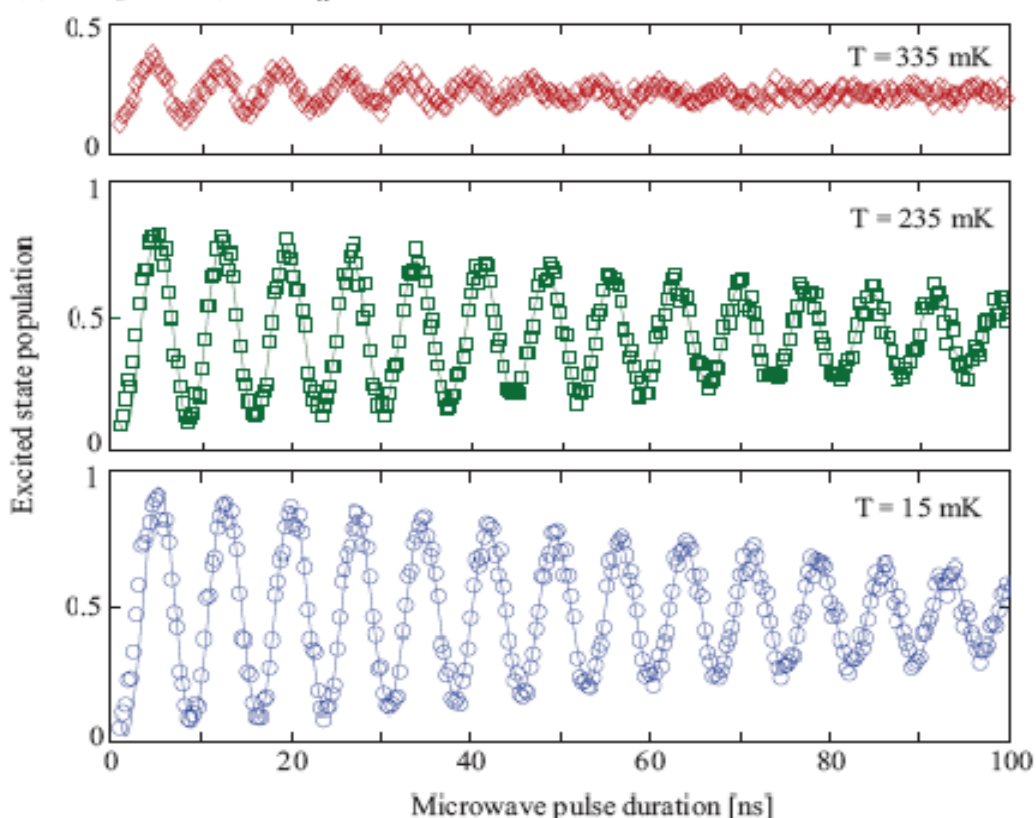
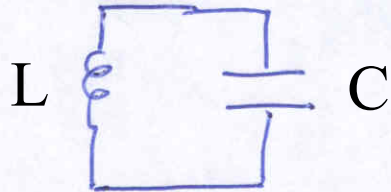


FIG. 2: (a) Rabi oscillations observed in Nb-based sample #1 with SiO₂ insulation and (b) in Al-based sample #2 featuring SiN_x insulation, at the indicated temperatures. Solid lines are a fits to exponentially decaying sine functions from which Rabi amplitude and decay time are extracted.

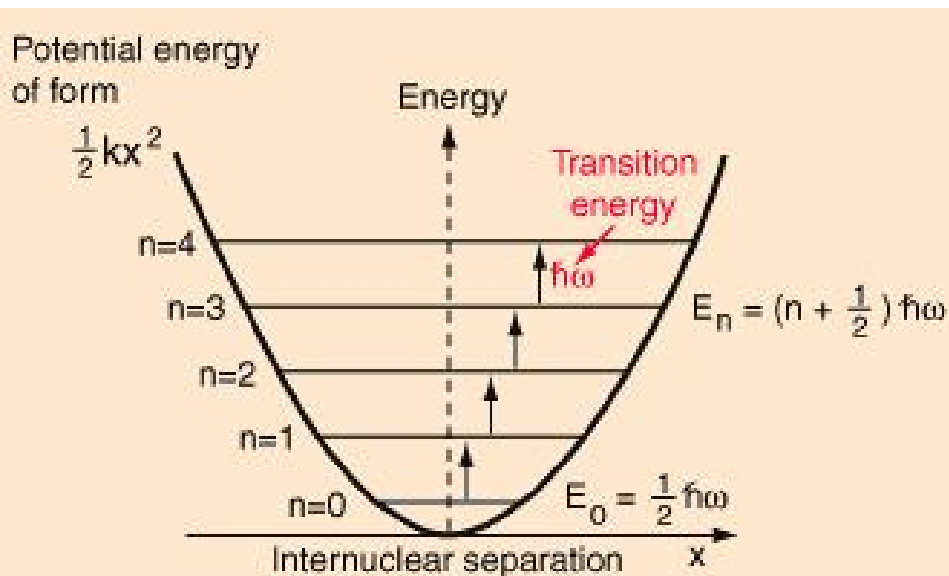
Simple electric circuit...



harmonic oscillator with resonant frequency

$$\omega_0 = 1 / \sqrt{LC}$$

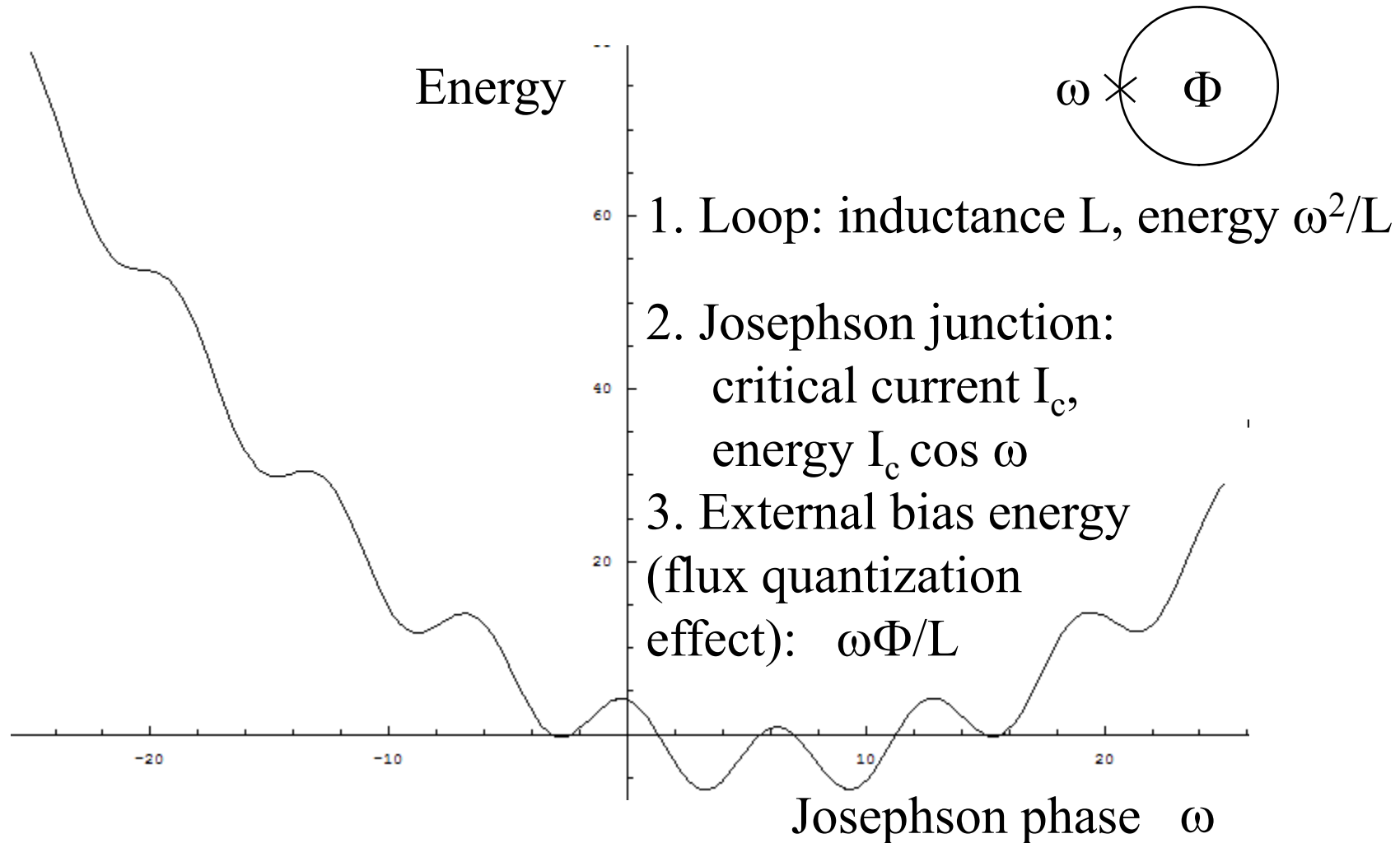
Quantum mechanically, like a kind of atom (with harmonic potential):



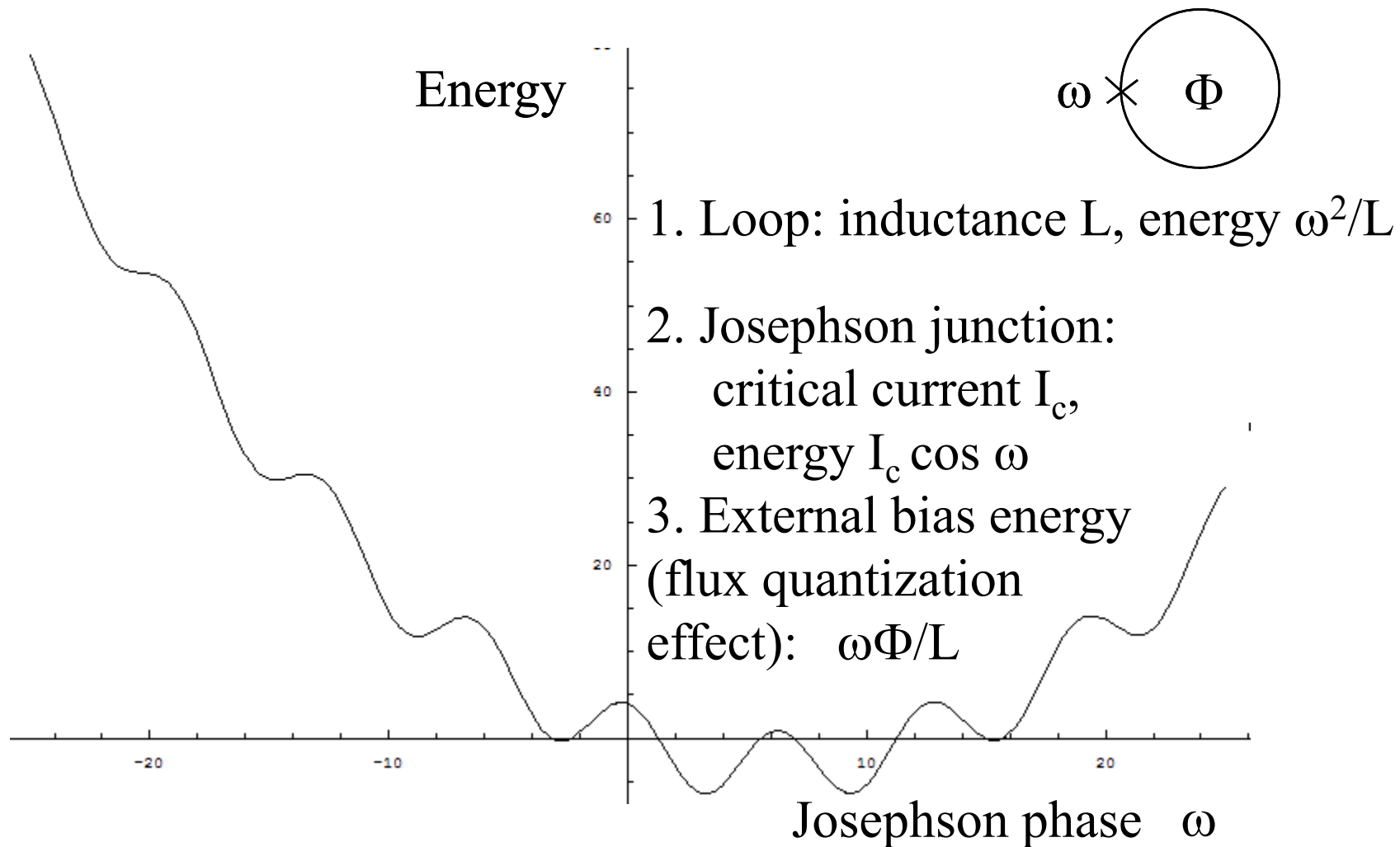
x is any circuit variable
(capacitor charge/current/voltage,
Inductor flux/current/voltage)

That is to say, it is a
“macroscopic” variable that is
being quantized.

Textbook (classical) SQUID characteristic: the “washboard”

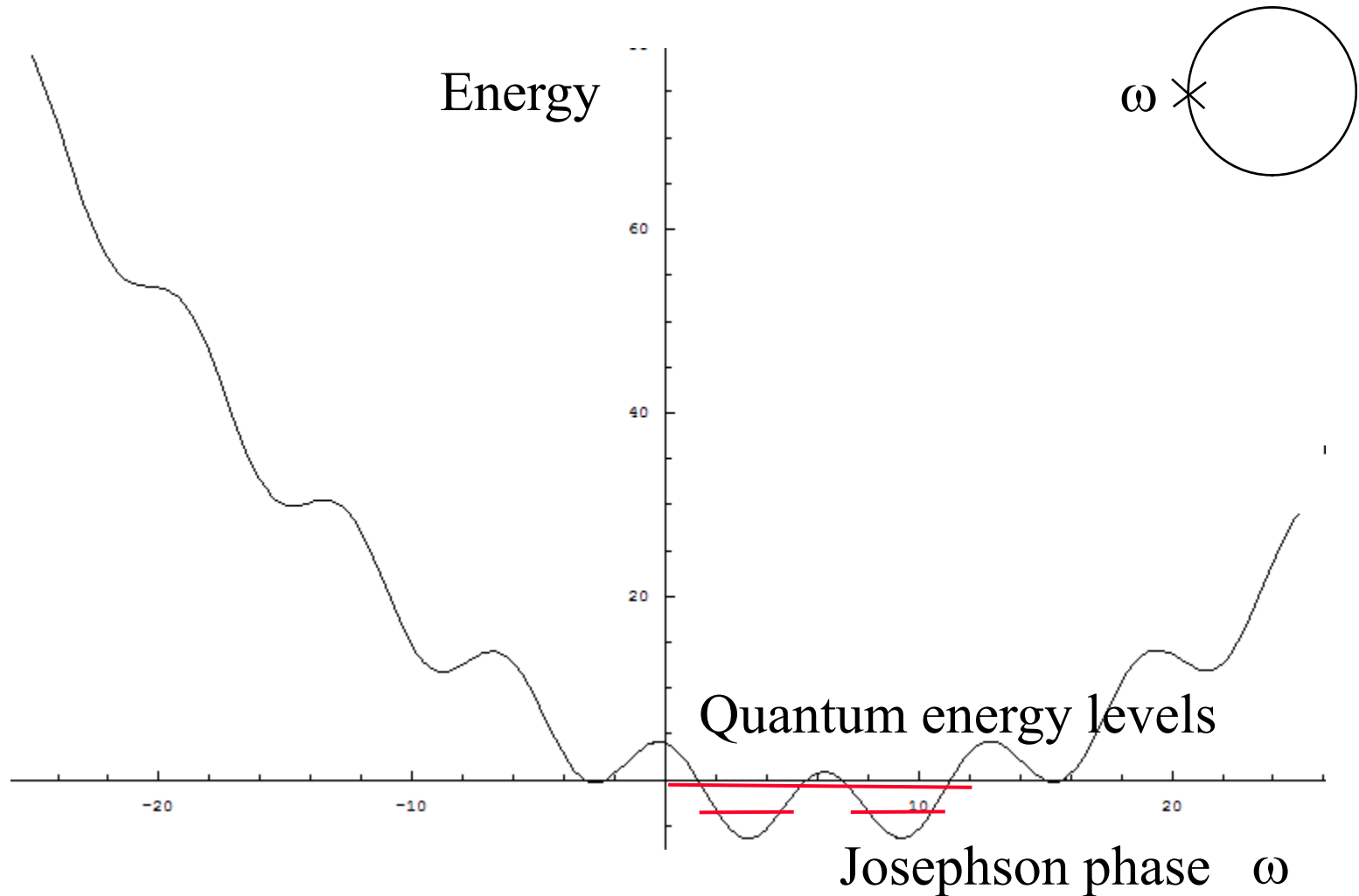


Textbook (classical) SQUID characteristic: the “washboard”



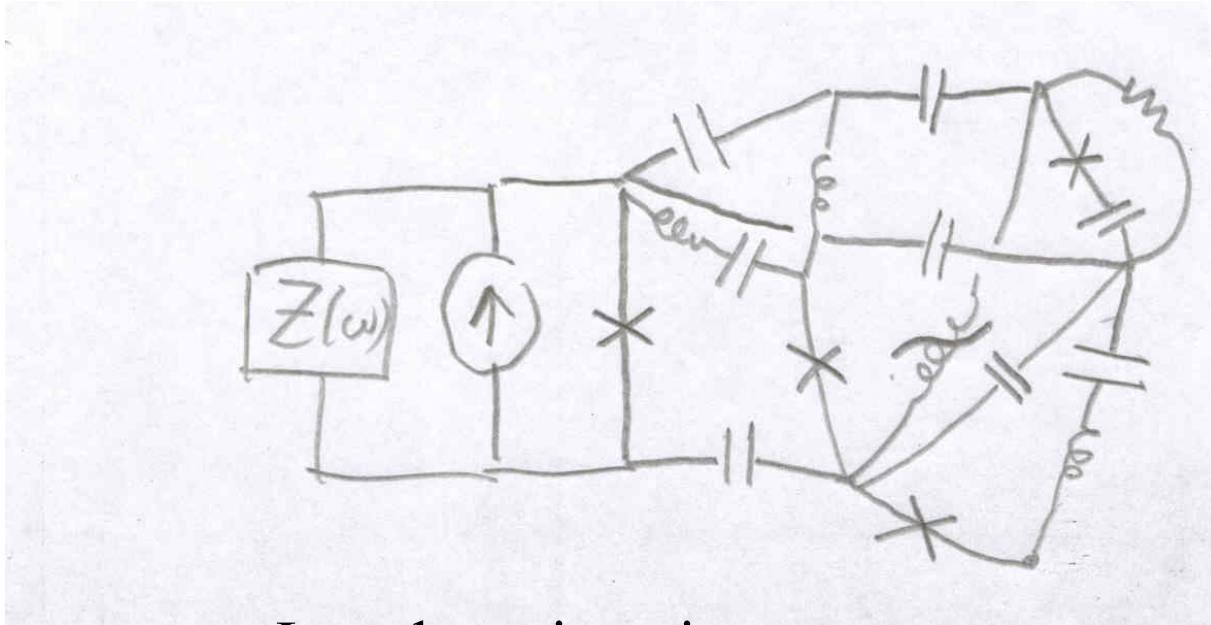
Junction capacitance C , plays role of particle mass

Quantum SQUID characteristic: the “washboard”



Junction capacitance C , plays role of particle mass

But we will need to learn to deal with...

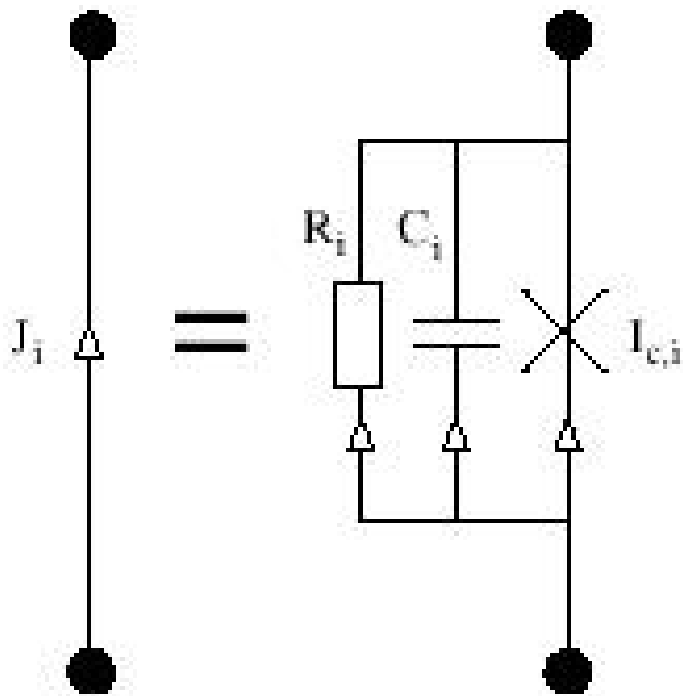


- Josephson junctions
- current sources
- resistances and impedances
- mutual inductances
- non-linear circuit elements?

G. Burkard, R. H. Koch, and D. P. DiVincenzo, "Multi-level quantum description of decoherence in superconducting flux qubits," Phys. Rev. B **69**, 064503 (2004); cond-mat/0308025.

Josephson junction circuits

Practical Josephson junction is a combination of three electrical elements:



Ideal Josephson junction (x in circuit):
current controlled by difference in superconducting phase φ across the tunnel junction:

$$\mathbf{I}_J = \mathbf{I}_C \sin \varphi$$

Completely new electrical circuit element, right?

not really...

What's an inductor (linear or nonlinear)?

$$\Phi = LI, \quad (\text{instantaneous})$$

$$I = L^{-1}\Phi$$

$$I = L^{-1}(\Phi)$$

Φ is the magnetic flux produced by the inductor

$$\dot{\Phi} = V$$

(Faraday)

Ideal Josephson junction:

$$\mathbf{I}_J = \mathbf{I}_c \sin\varphi$$

φ is the superconducting phase difference across the barrier

$$\frac{\Phi_0}{2\pi} \dot{\varphi} = V$$

(Josephson's second law)

$$\Phi_0 = h / e \quad \text{flux quantum}$$

not really...

What's an inductor (linear or nonlinear)?

$$\Phi = LI,$$

$$I = L^{-1}\Phi$$

$$I = L^{-1}(\Phi)$$

Φ is the magnetic flux produced by the inductor

$$\dot{\Phi} = V$$

(Faraday)

Ideal Josephson junction:

$$\mathbf{I}_J = \mathbf{I}_c \sin\varphi$$

φ is the superconducting phase difference across the barrier

$$\frac{\Phi_0}{2\pi} \dot{\varphi} = V$$

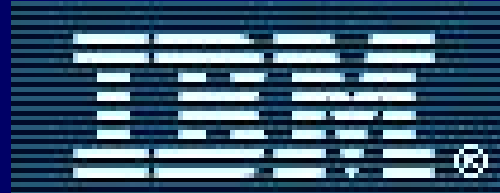
(Josephson's second law)

Phenomenologically, Josephson junctions are non-linear inductors.

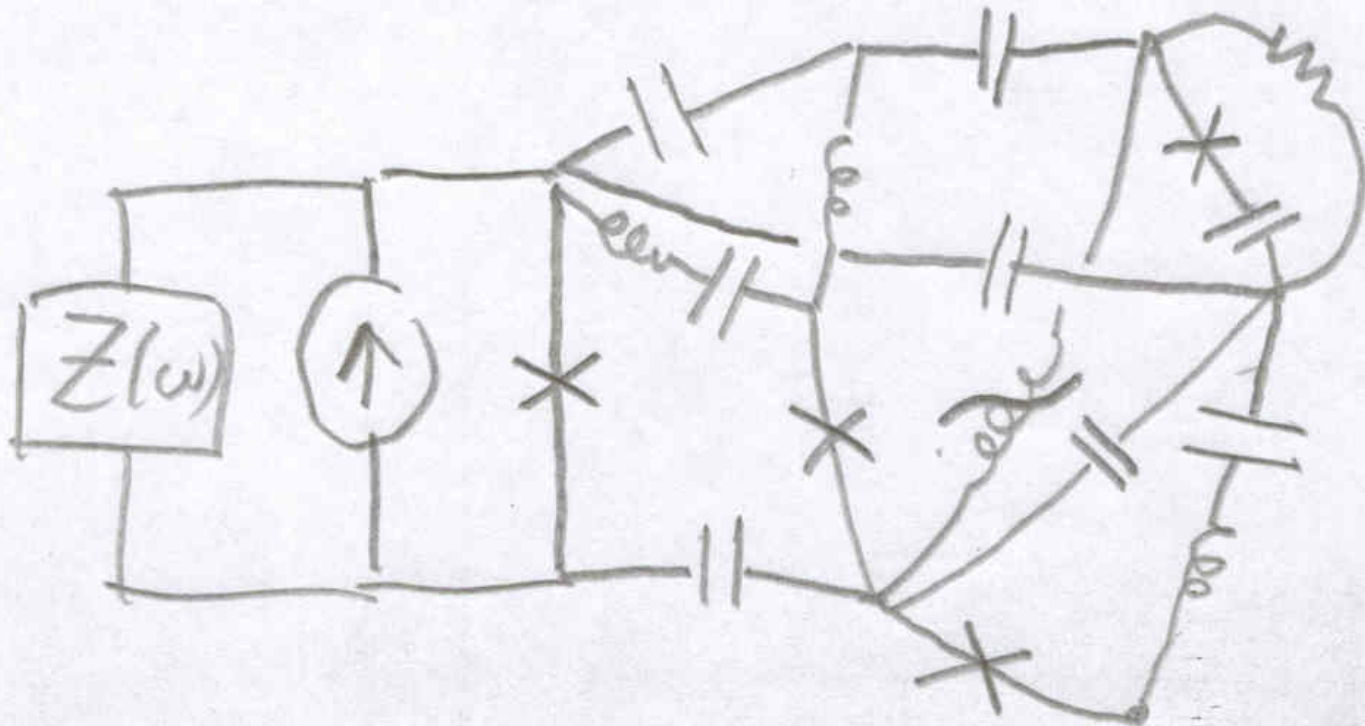
Superconducting Qubits

David DiVincenzo, IBM

Ann Arbor Summer School, 6/2008



So, we now do the systematic quantum theory



Graph formalism

1. Identify a “tree” of the graph – maximal subgraph containing all nodes and no loops

Branches not in tree are called “*chords*”; each chord completes a *loop*

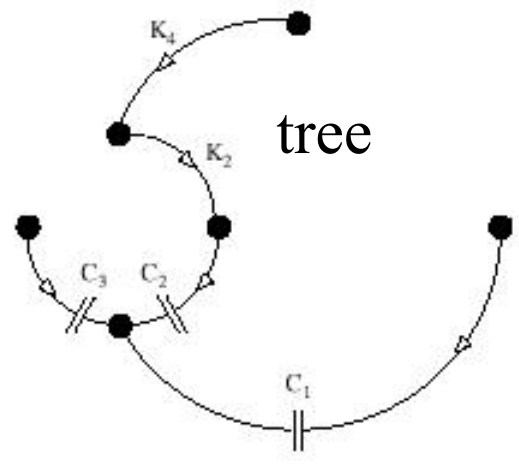
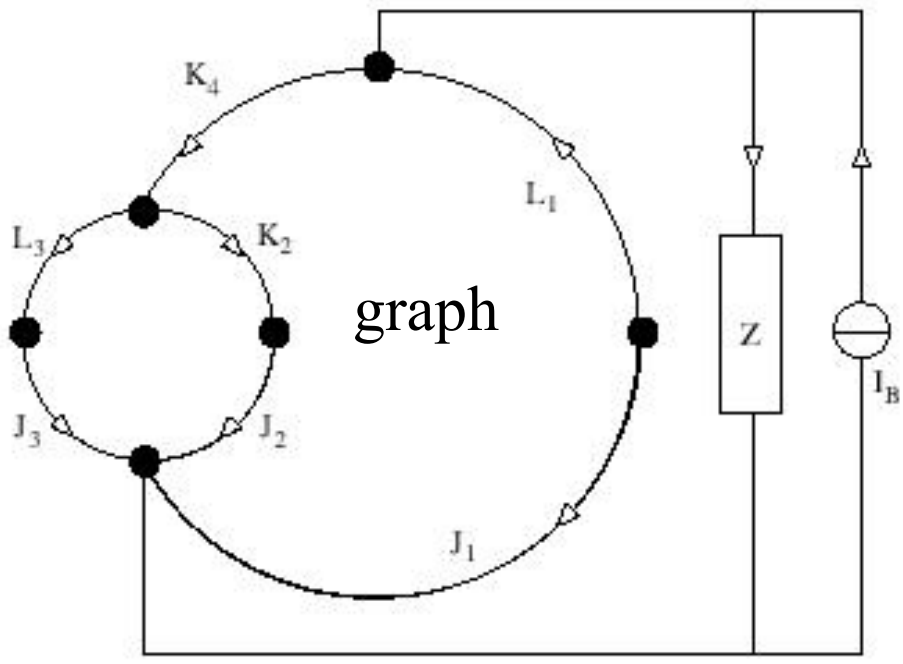


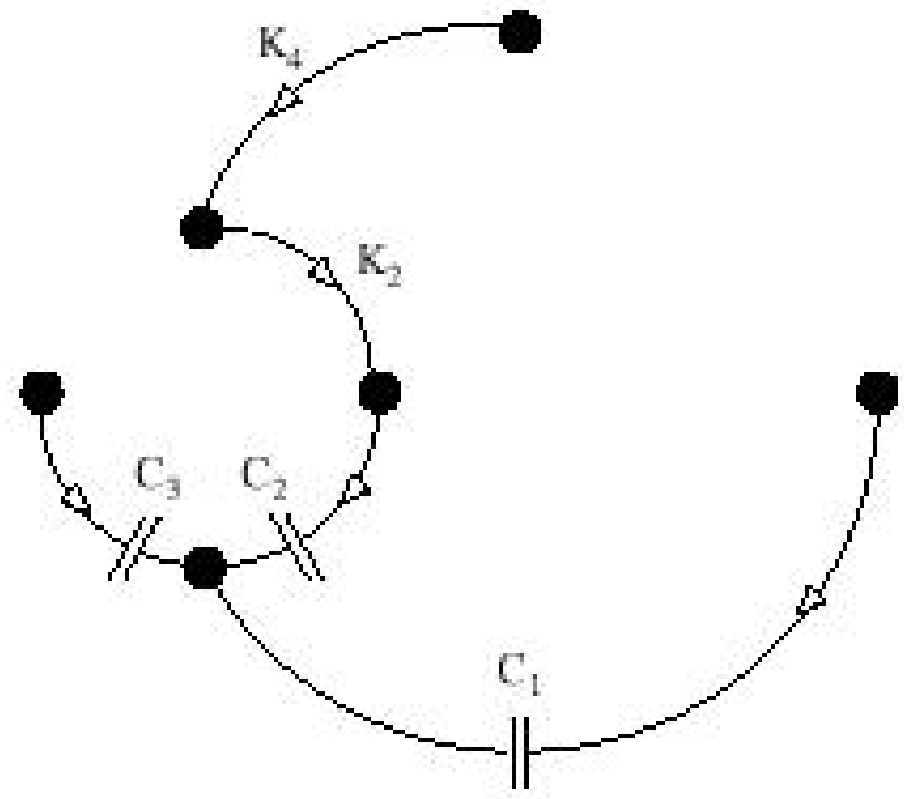
FIG. 1: The IBM qubit. This is an example of a network graph with 6 nodes and 15 branches. Each thick line represents a Josephson element, i.e. three branches in parallel, see Figure 2. Thin lines represent simple two-terminal elements, such as linear inductors (L, K), external impedances (Z), and current sources (I_B).

for the circuit shown in Figure 1. A tree is a spanning all nodes and no loop. Here, we choose a tree that contains all capacitors (C), some inductors (K), and the current source (I_B) or external impedances (Z).

graph formalism, continued

e.g.,
$$\mathbf{F}_{CL} = \begin{pmatrix} 1 & 0 \\ -1 & 1 \\ 0 & -1 \end{pmatrix}$$

NB: this introduces
submatrix of F labeled
by branch type



Circuit equations in the graph formalism:

Kirchhoff's current laws:

$$\mathbf{F}^{(C)} \mathbf{I} = \mathbf{0}$$

\mathbf{V} : branch voltages

\mathbf{I} : branch currents

Φ : external fluxes threading loops

Kirchhoff's voltage laws:

$$\mathbf{F}^{(L)} \mathbf{V} = \dot{\Phi}$$

Equation of motion of a complex circuit:

$$\mathbf{C}\ddot{\varphi} = -\mathbf{L}_J^{-1}\sin\varphi - \mathbf{R}^{-1}\dot{\varphi} - \mathbf{M}_0\varphi - \mathbf{M}_d * \varphi - \frac{2\pi}{\Phi_0}\mathbf{N}\Phi_x - \frac{2\pi}{\Phi_0}\mathbf{S}\mathbf{I}_B$$

small

The lossless parts of this equation arise from a simple Hamiltonian:

H; $U = \exp(iHt)$

$$\frac{1}{2}\mathbf{Q}_C^T \mathbf{C}^{-1} \mathbf{Q}_C + U(\varphi)$$

$$U(\varphi) = -\sum_i L_{J;i}^{-1} \cos \varphi_i$$

$$+ \frac{1}{2}\varphi^T \mathbf{M}_0 \varphi + \frac{2\pi}{\Phi_0}\varphi^T (\mathbf{N}\Phi_x + \mathbf{S}\mathbf{I}_B)$$

Burkard, Koch, DiVincenzo,
PRB (2004).

the equation of motion (continued):

$$\mathbf{C}\ddot{\varphi} = -\mathbf{L}_J^{-1}\sin\varphi - \mathbf{R}^{-1}\dot{\varphi} - \mathbf{M}_0\varphi - \mathbf{M}_d * \varphi - \frac{2\pi}{\Phi_0}\mathbf{N}\Phi_x - \frac{2\pi}{\Phi_0}\mathbf{S}\mathbf{I}_B$$

$$\mathbf{M}_0 = \mathbf{F}_{CL}\tilde{\mathbf{L}}_L^{-1}\bar{\mathbf{L}}\mathbf{L}_{LL}^{-1}\mathbf{F}_{CL}^T,$$

$$\mathbf{N} = \mathbf{F}_{CL}\tilde{\mathbf{L}}_L^{-1}\bar{\mathbf{L}}\mathbf{L}_{LL}^{-1},$$

$$\mathbf{M}_d(\omega) = \bar{\mathbf{m}}\bar{\mathbf{L}}_Z^{-1}(\omega)\bar{\mathbf{m}}^T,$$

$$\bar{\mathbf{m}} = \mathbf{F}_{CZ} - \mathbf{F}_{CL}(\mathbf{L}_{LL}^{-1})^T\bar{\mathbf{F}}_{KL}^T\tilde{\mathbf{L}}_K^T\mathbf{F}_{KZ}$$

$$\mathbf{S} = \mathbf{F}_{CB} - \mathbf{F}_{CL}(\mathbf{L}_{LL}^{-1})^T\bar{\mathbf{F}}_{KL}^T\tilde{\mathbf{L}}_K^T\mathbf{F}_{KB}$$

All are complicated but straightforward functions of the topology (F matrices) and the inductance matrix

the equation of motion (continued):

$$\mathbf{C}\ddot{\varphi} = -\mathbf{L}_J^{-1}\sin\varphi - \mathbf{R}^{-1}\dot{\varphi} - \mathbf{M}_0\varphi - \mathbf{M}_d * \varphi - \frac{2\pi}{\Phi_0}\mathbf{N}\Phi_x - \frac{2\pi}{\Phi_0}\mathbf{S}\mathbf{I}_B$$

small

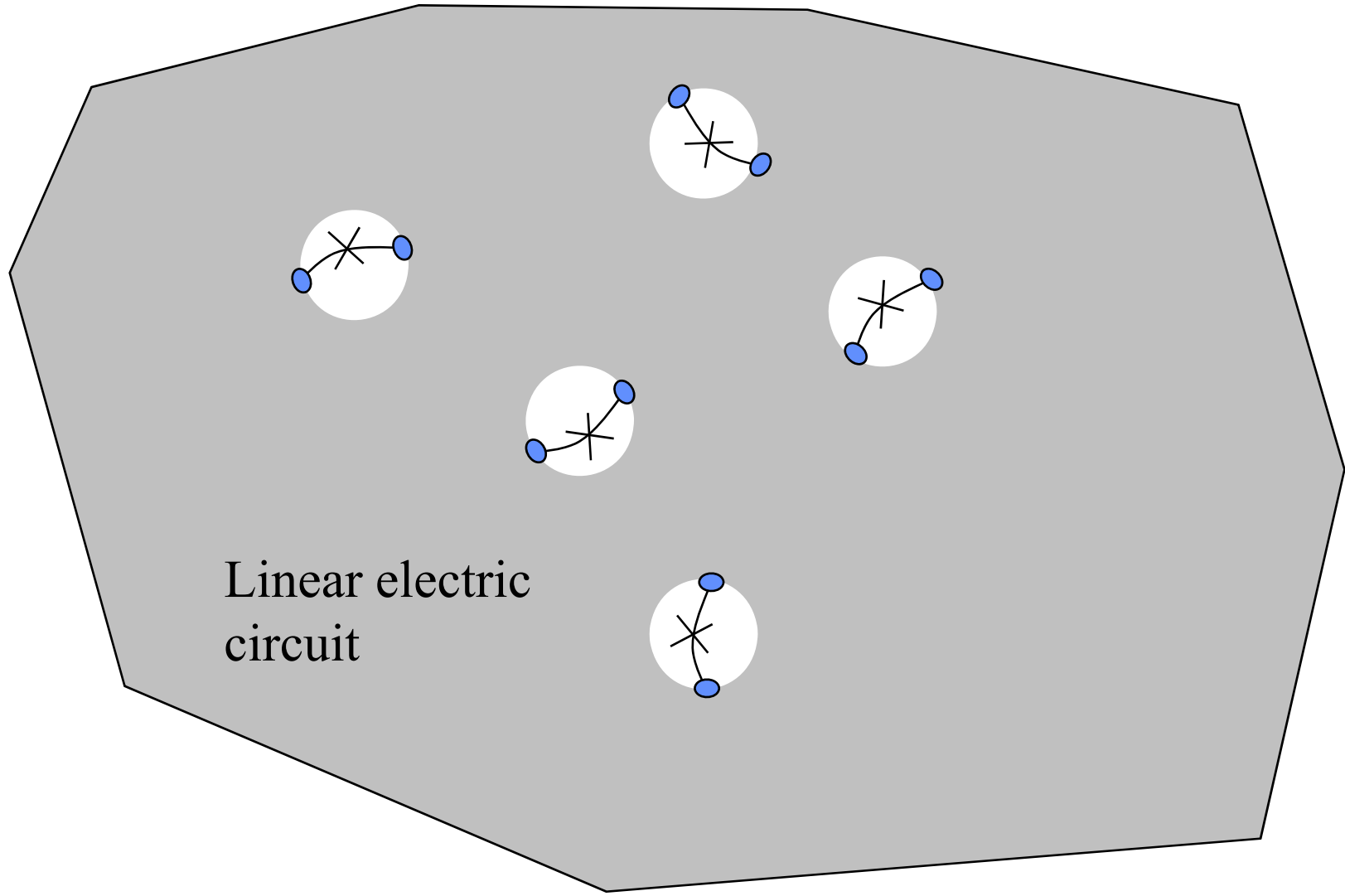
$$\mathbf{M}_0 = \mathbf{F}_{CL}\tilde{\mathbf{L}}_L^{-1}\bar{\mathbf{L}}\mathbf{L}_{LL}^{-1}\mathbf{F}_{CL}^T,$$

$$\mathbf{N} = \mathbf{F}_{CL}\tilde{\mathbf{L}}_L^{-1}\bar{\mathbf{L}}\mathbf{L}_{LL}^{-1}, \dots$$

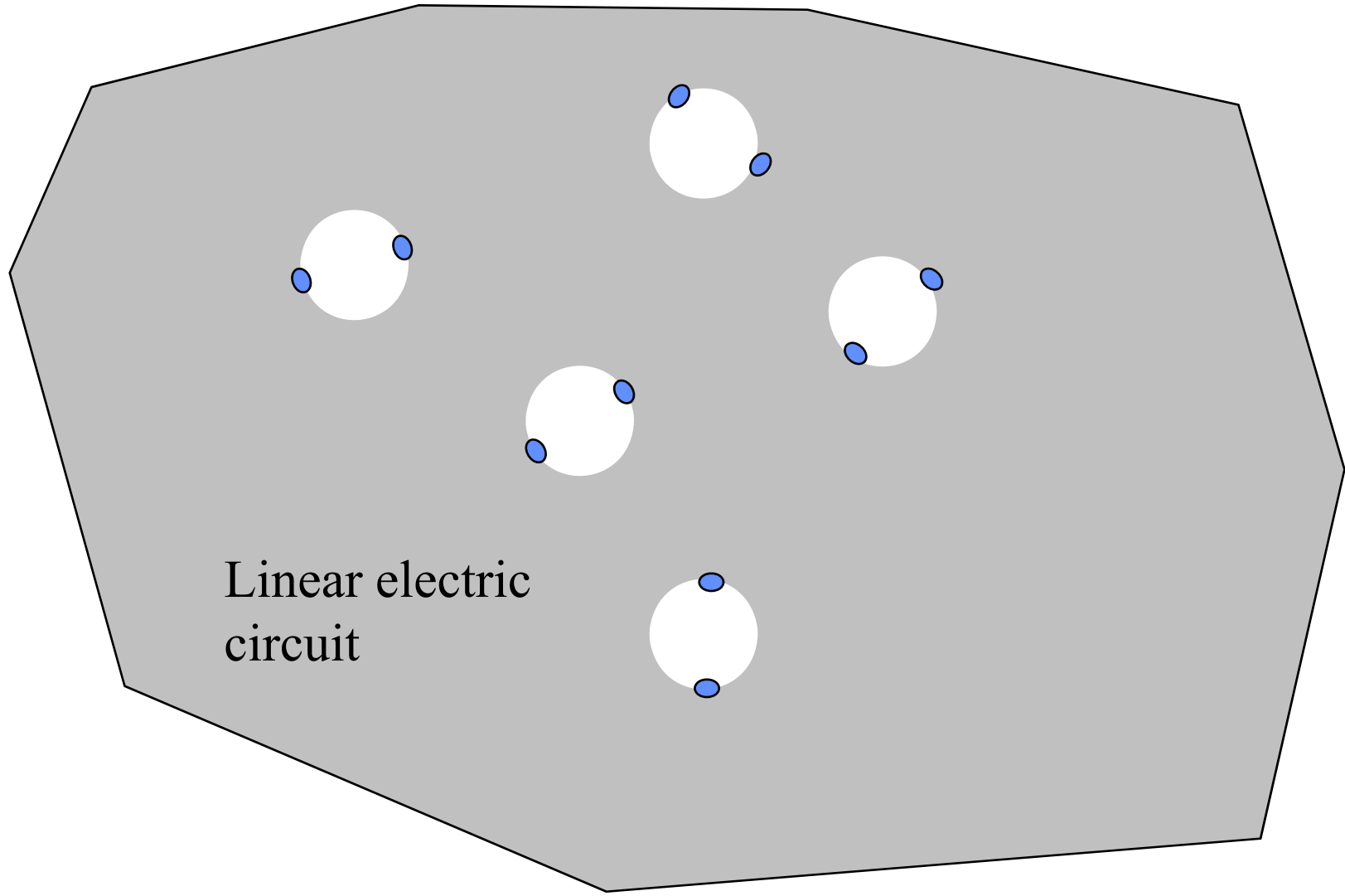
$$\begin{aligned} \bar{\mathbf{N}}(\omega = 0) = \mathbf{F}_{CL} & \left[\mathbf{1}_L + \mathbf{L}^{-1}\mathbf{L}_{LK} \left(\mathbf{L}_K - \mathbf{L}_{LK}^T \mathbf{L}^{-1} \mathbf{L}_{LK} \right)^{-1} \right. \\ & \left. \left(\mathbf{1}_K - \mathbf{L}_K \left(\mathbf{F}_{KL} - \mathbf{L}_K^{-1} \mathbf{L}_{LK}^T \right) \mathbf{L}^{-1} \mathbf{L}_{LK} \left(\mathbf{L}_K - \mathbf{L}_{LK}^T \mathbf{L}^{-1} \mathbf{L}_{LK} \right)^{-1} \right)^{-1} \mathbf{L}_K \left(\mathbf{F}_{KL} - \mathbf{L}_K^{-1} \mathbf{L}_{LK}^T \right) \right] \\ & \left[\mathbf{L} - \mathbf{L}_{LK} \mathbf{L}_K^{-1} \mathbf{L}_{LK}^T + \mathbf{F}_{KL}^T \left(\mathbf{1}_K - \mathbf{L}_K \left(\mathbf{F}_{KL} - \mathbf{L}_K^{-1} \mathbf{L}_{LK}^T \right) \mathbf{L}^{-1} \mathbf{L}_{LK} \left(\mathbf{L}_K - \mathbf{L}_{LK}^T \mathbf{L}^{-1} \mathbf{L}_{LK} \right)^{-1} \right)^{-1} \mathbf{L}_K \left(\mathbf{F}_{KL} - \mathbf{L}_K^{-1} \mathbf{L}_{LK}^T \right) \right]^{-1}. \end{aligned} \quad (89)$$

Straightforward (but complicated!) functions of the topology (F matrices) and the inductance matrix

The physics of the coupling matrices

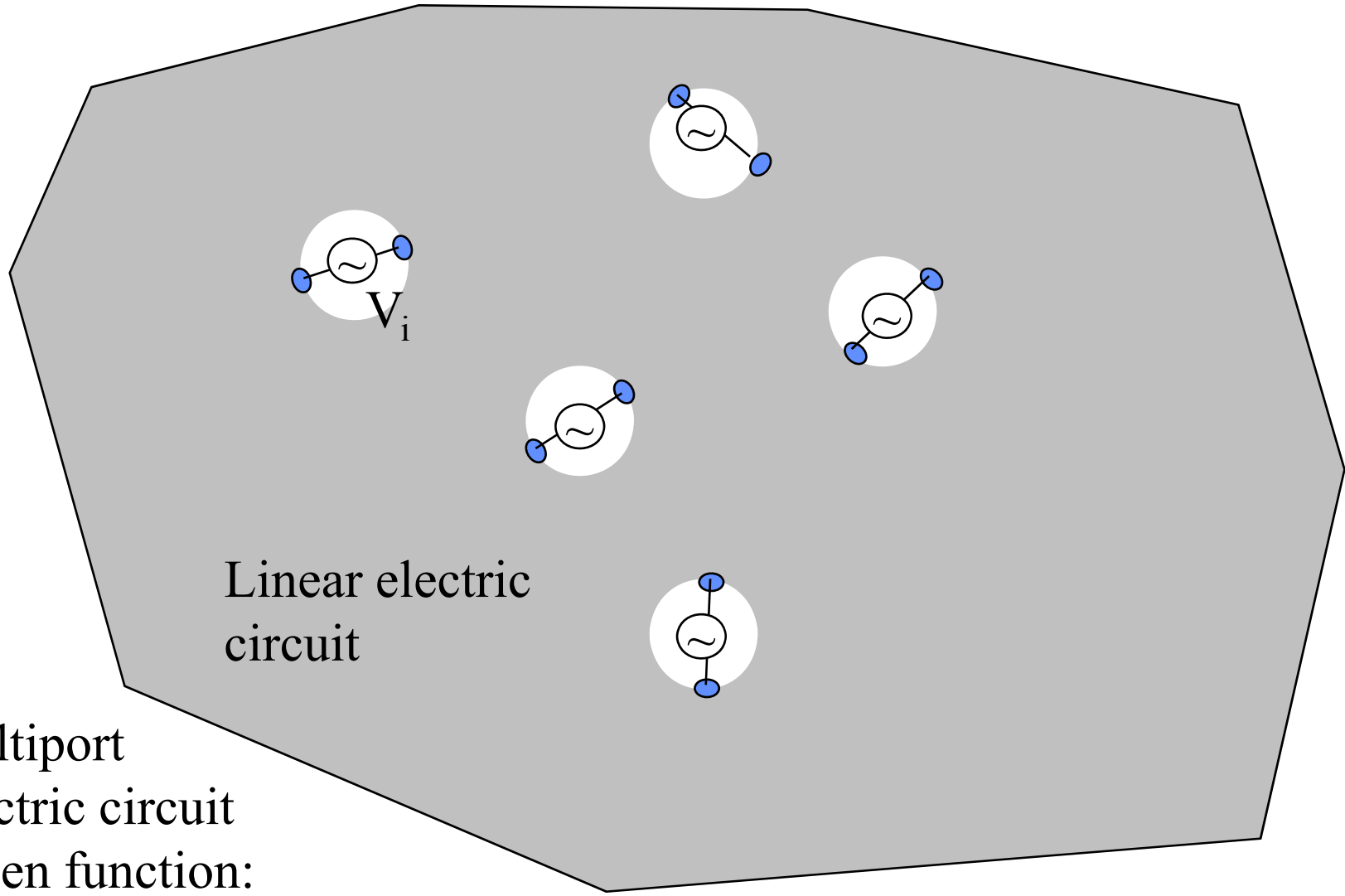


The physics of the coupling matrices



Cut out the Josephson junctions...

The physics of the coupling matrices



Multiport
Electric circuit
Green function:

$$I_j(\omega) = Y_{ij}(\omega) V_i(\omega), \quad Y_{ij}(\omega) = \frac{1}{i\omega} (L^{-1})_{ij} + \dots = \frac{\vec{M}_0}{i\omega} + \dots$$

the equation of motion (continued):

$$\mathbf{C}\ddot{\varphi} = -\mathbf{L}_J^{-1}\sin\varphi - \mathbf{R}^{-1}\dot{\varphi} - \mathbf{M}_0\varphi - \mathbf{M}_d * \varphi - \frac{2\pi}{\Phi_0}\mathbf{N}\Phi_x - \frac{2\pi}{\Phi_0}\mathbf{S}\mathbf{I}_B$$

The lossy parts of this equation arise from a bath Hamiltonian,
Via a Caldeira-Leggett treatment:

$$\mathcal{H} = \mathcal{H}_S + \mathcal{H}_B + \mathcal{H}_{SB},$$

$$\mathcal{H}_B = \frac{1}{2} \sum_{\alpha} \left(\frac{p_{\alpha}^2}{m_{\alpha}} + m_{\alpha} \omega_{\alpha}^2 x_{\alpha}^2 \right),$$

$$\mathcal{H}_{SB} = \mathbf{m} \cdot \varphi \sum_{\alpha} c_{\alpha} x_{\alpha} + \Delta U(\varphi),$$

Connecting Cadeira Leggett to circuit theory:

$$\begin{aligned}
 \mathcal{H} &= \mathcal{H}_S + \mathcal{H}_B + \mathcal{H}_{SB}, & \mathbf{M}_d(\omega) &= \mu K(\omega) \mathbf{m} \mathbf{m}^T, \\
 \mathcal{H}_B &= \frac{1}{2} \sum_{\alpha} \left(\frac{p_{\alpha}^2}{m_{\alpha}} + m_{\alpha} \omega_{\alpha}^2 x_{\alpha}^2 \right), & K(\omega) &= \bar{\mathbf{L}}_Z^{-1}(\omega), \\
 \mathcal{H}_{SB} &= \mathbf{m} \cdot \boldsymbol{\varphi} \sum_{\alpha} c_{\alpha} x_{\alpha} + \Delta U(\boldsymbol{\varphi}), & \mu &= |\bar{\mathbf{m}}|^2, \\
 & & \mathbf{m} &= \bar{\mathbf{m}} / \sqrt{\mu} = \bar{\mathbf{m}} / |\bar{\mathbf{m}}|,
 \end{aligned}$$

$$J(\omega) = \frac{\pi}{2} \sum_{\alpha} \frac{c_{\alpha}^2}{m_{\alpha} \omega_{\alpha}} \delta(\omega - \omega_{\alpha})$$

$$J(\omega) = -\mu \left(\frac{\Phi_0}{2\pi} \right)^2 \text{Im} K(\omega)$$

Overview of what we've accomplished:

We have a systematic derivation of a general system-bath Hamiltonian. From this we can proceed to obtain:

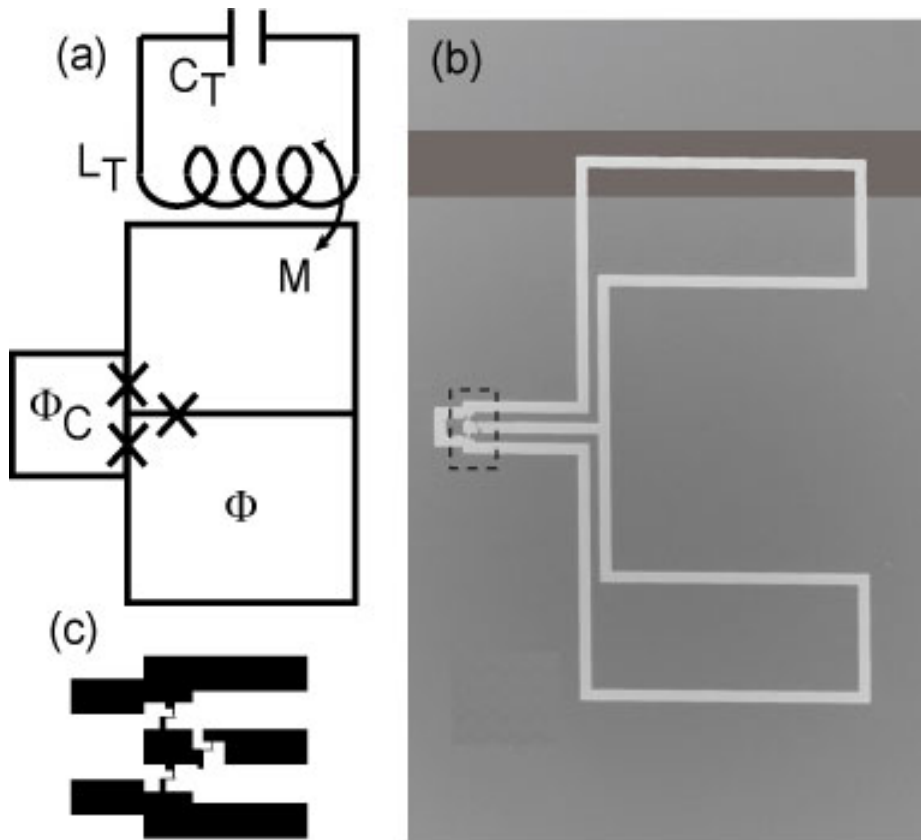
- system master equation
- spin-boson approximation (two level)
- Born-Markov approximation -> Bloch Redfield theory
- golden rule (decay rates)
- leakage rates

For example:

$$\frac{1}{T_1} = \left(\frac{\Delta}{\omega_{01}} \right)^2 |\Delta \boldsymbol{\varphi} \cdot \mathbf{m}|^2 J(\omega_{01}) \coth \frac{\omega_{01}}{2k_B T}, \quad (131)$$

$$\frac{1}{T_\phi} = \left(\frac{\epsilon}{\omega_{01}} \right)^2 |\Delta \boldsymbol{\varphi} \cdot \mathbf{m}|^2 \frac{J(\omega)}{\omega} \Big|_{\omega \rightarrow 0} 2k_B T. \quad (132)$$

IBM Josephson junction qubit



“qubit” = circulation of electric current in one direction or another (????)

Low-bandwidth control scheme for an oscillator stabilized Josephson qubit

R. H. Koch, J. R. Rozen, G. A. Keefe, F. M. Milliken, C. C. Tsuei, J. R. Kirtley, and D. P. DiVincenzo

IBM Watson Research Ctr., Yorktown Heights, NY 10598 USA

(Dated: November 16, 2004)

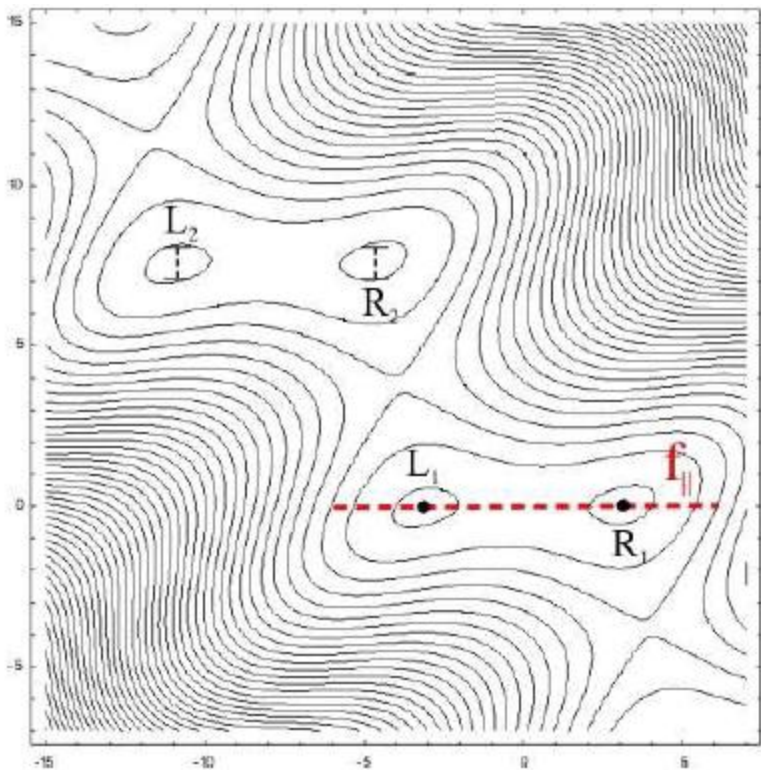


FIG. 2: Contour plot of the potential $U'(f)$ on the S line for the external fluxes $\Phi_c = 0.36\Phi_0$ and $\Phi = \Phi_0$. The red dashed line indicates the “slow” direction f_{\parallel} . Along this direction the potential is a symmetric double well, with the two relevant minima of the potential indicated by dots. The bars show the spatial extension of the wave function, in the vicinity of the minima, in the “fast” direction f_{\perp} with the smallest curvature of the potential.

small-loop noise: gradiometrically protected

Large-loop noise: bad, but heavily filtered

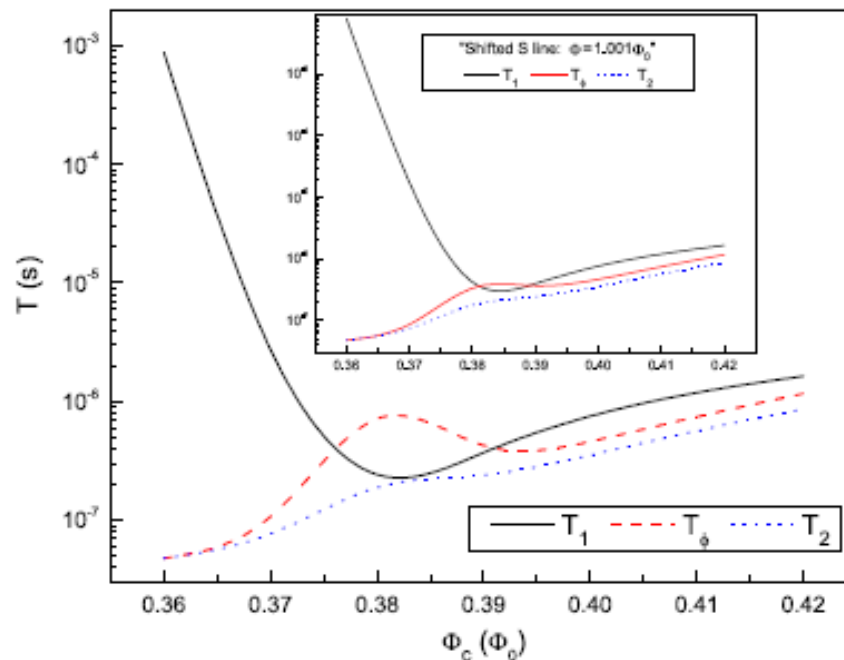


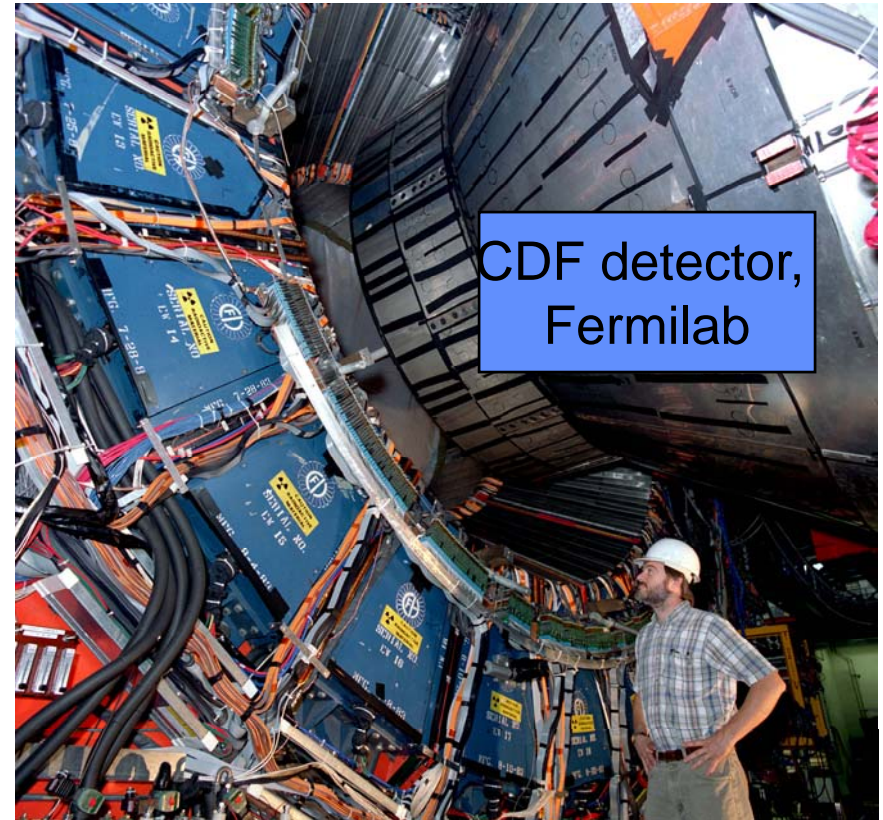
FIG. 20: The total relaxation, dephasing and decoherence times (T_1 , T_{ϕ} and T_2 , respectively) along the S line. We can see that T_{ϕ} (T_1) strongly increases (decreases) as a function of Φ_c . These facts cause there to be a window of desirable operating parameters for the qubit.

“Charge”, “Phase”, and “Flux” Qubits?

“No power is required to perform computation.”
CH Bennett

“Quantum computers can operate autonomously.”
N Margolus

(inventor of “computronium”)





Efficient one- and two-qubit pulsed gates for an oscillator stabilized Josephson qubit

Frederico Brito, David P. DiVincenzo, Matthias Steffen
and Roger H. Koch

Efficient one- and two-qubit pulsed gates for an oscillator stabilized Josephson qubit

Frederico Brito, David P. DiVincenzo, Roger H. Koch*, and Matthias Steffen
IBM T. J. Watson Research Center, P. O. Box 218, Yorktown Heights, NY 10598 USA
(Dated: September 10, 2007)

arXiv:0709.1478v1 [quant-ph] 10 Sep 2007

New J. Phys. 2008



R. Koch
1950-2007

Fault-Tolerant Computing With Biased-Noise Superconducting Qubits

P. Aliferis^{††}, F. Brito^{††}, D. P. DiVincenzo[†], J. Preskill[‡], M. Steffen[†], and B. M. Terhal[†]

June 2, 2008

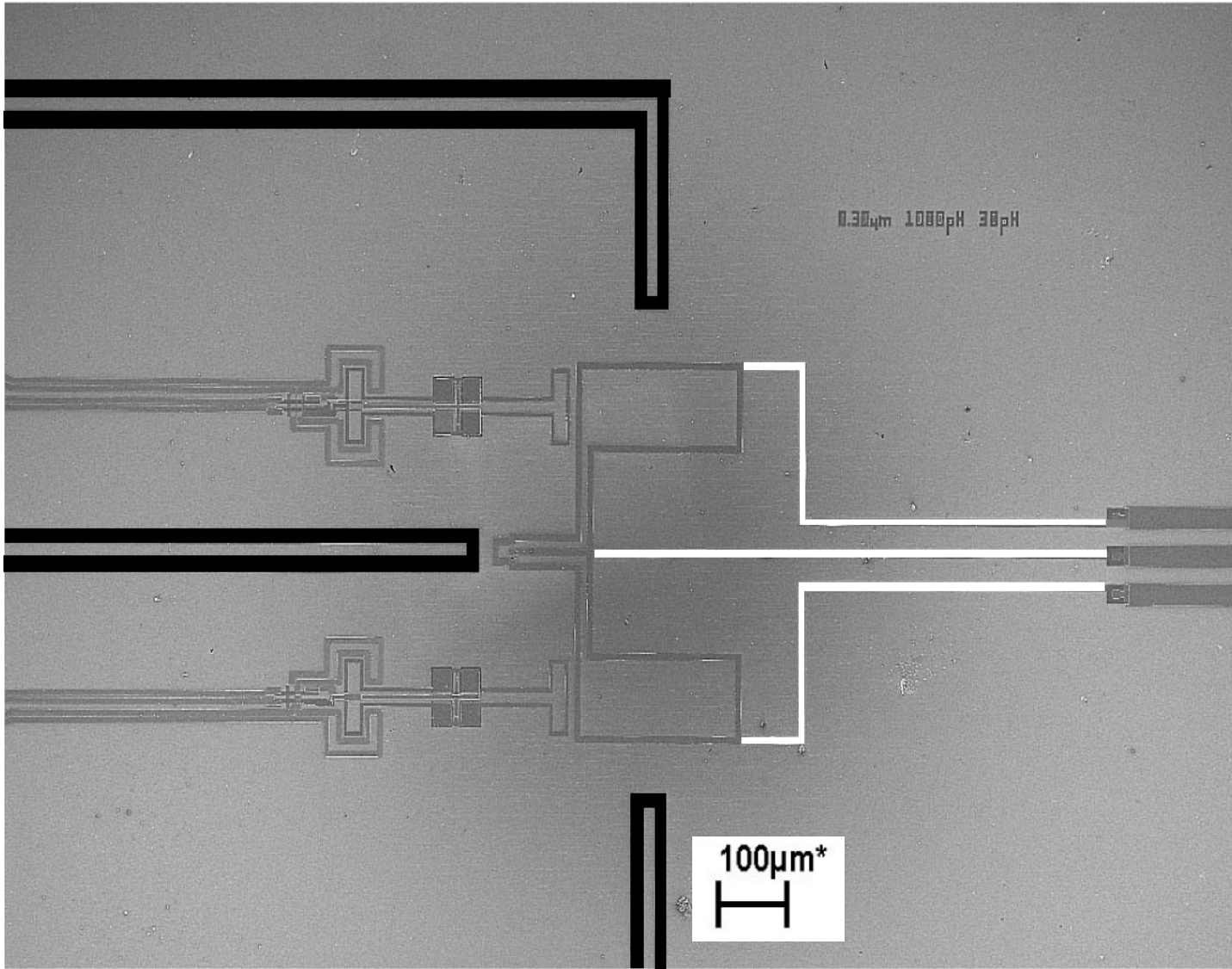
Abstract

We present a simple universal scheme of pulsed operations for the IBM oscillator-stabilized flux qubit comprising the controlled- σ_x (CPHASE) gate, single-qubit preparations and measurements. Based on numerical simulations, we argue that the error rates for these operations can be as low as about .5% and that noise is highly biased, with phase errors being stronger than all other types of errors by a factor of nearly 10^3 . In contrast, the design of a controlled- σ_x (CNOT) gate for this system with an error rate of less than about 1.2% seems extremely challenging. We propose a special encoding which exploits the noise bias allowing us to implement a *logical* CNOT gate where phase errors and all other types of errors have nearly balanced rates of about .4%. The basic principles underlying our scheme can also find application in other solid-state qubits, strengthening our hope that the fidelities needed for fault-tolerant quantum computation can be achieved with integrated circuits.

After years of painstaking labor, superconducting qubits [1] are taking shape as viable elements for the construction of a scalable quantum computer. Since the initial demonstrations of coherent quantum dynamics in superconducting qubits [2, 4, 3, 5], it has been recognized that these systems have great potential versatility [6, 7, 8], so that one can genuinely envision a quantum-computing integrated circuit emerging from this research. However, no clear way forward has been announced, owing largely to one undeniable feature of large-scale quantum computation: it will require a very high degree of fidelity in the execution of quantum operations, much higher than has been reported in any present experiments.

How high a fidelity, or how low an error rate, will be needed? On the basis of fundamental early theoretical work [9, 10, 11], lip service is frequently paid to a necessary universal set of operations containing the two-qubit controlled- σ_x (CNOT) gate, and a necessary “threshold” error rate in the 10^{-5} – 10^{-4} range. Some recent modeling for superconducting qubits [12, 13] suggests that such noise levels could conceivably be reached in the lab; however, in current experimental practice the ability even to reliably *detect* such small error rates, let alone to achieve them, is in fact very questionable.

In this paper, we will consider the possibility of constructing a universal set of operations for the IBM “Koch qubit” [14, 8]¹. Although our set of operations will not contain the CNOT gate, we will propose an encoding scheme for implementing *logical* CNOT gates which can then be used for fault-tolerant quantum computation. With this encoding, the fidelity requirements are relaxed, and the error rates needed for



$$I_c = 1.3 \mu\text{A}$$

$$L_1 = 32 \text{ pH}$$

$$L_3 = 680 \text{ pH}$$

$$M_{1cf} = 0.8 \text{ pH}$$

$$M_{3flux} = 0.5 \text{ pH}$$

$$\omega_T = 2\pi \cdot 3.1 \text{ GHz}$$

$$Z_0 = 110 \Omega$$

$$L_T = 5.6 \text{ nH}$$

$$M_{qT} = 200 \text{ pH}$$

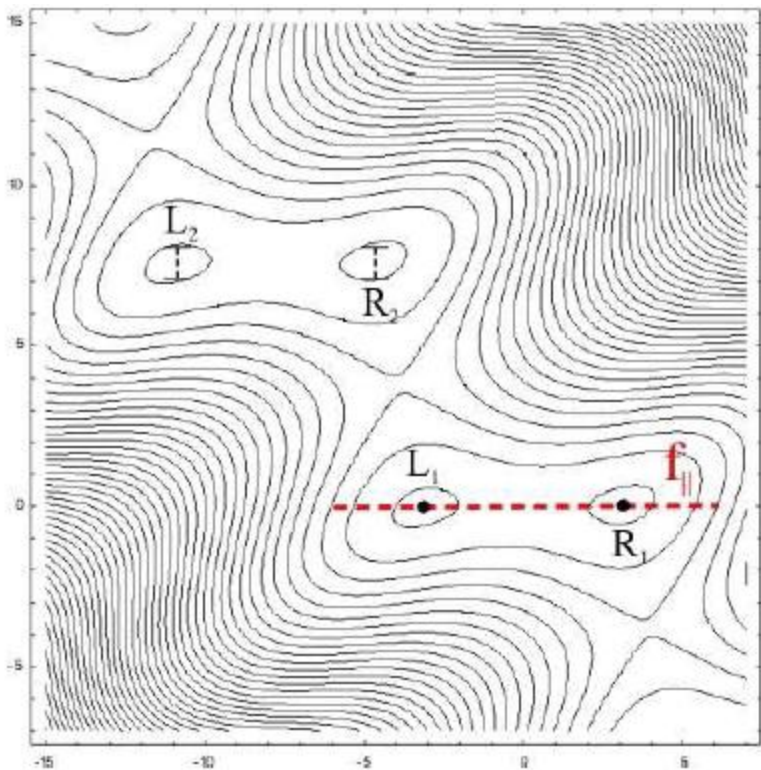


FIG. 2: Contour plot of the potential $U'(f)$ on the S line for the external fluxes $\Phi_c = 0.36\Phi_0$ and $\Phi = \Phi_0$. The red dashed line indicates the “slow” direction f_{\parallel} . Along this direction the potential is a symmetric double well, with the two relevant minima of the potential indicated by dots. The bars show the spatial extension of the wave function, in the vicinity of the minima, in the “fast” direction f_{\perp} with the smallest curvature of the potential.

small-loop noise: gradiometrically protected

Large-loop noise: bad, but heavily filtered

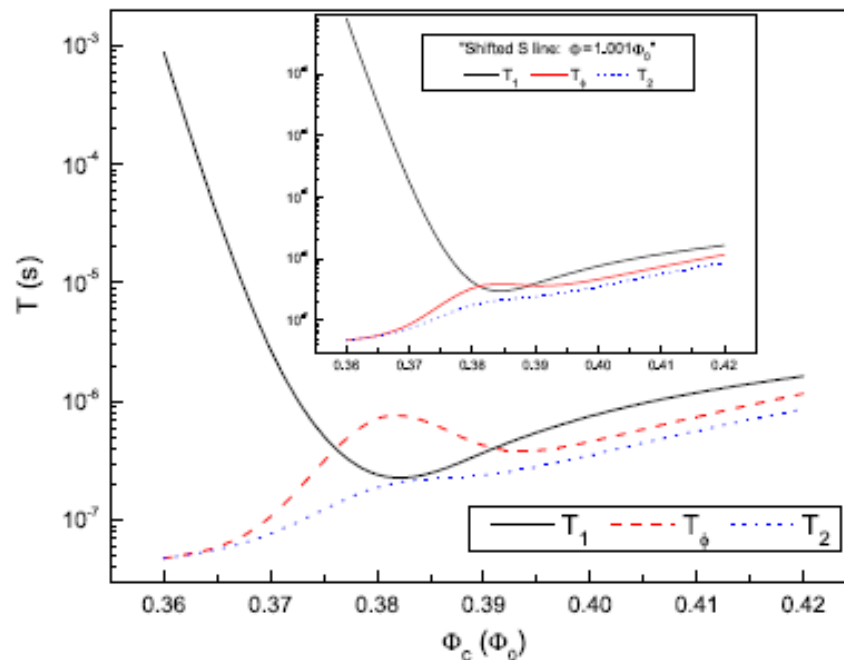
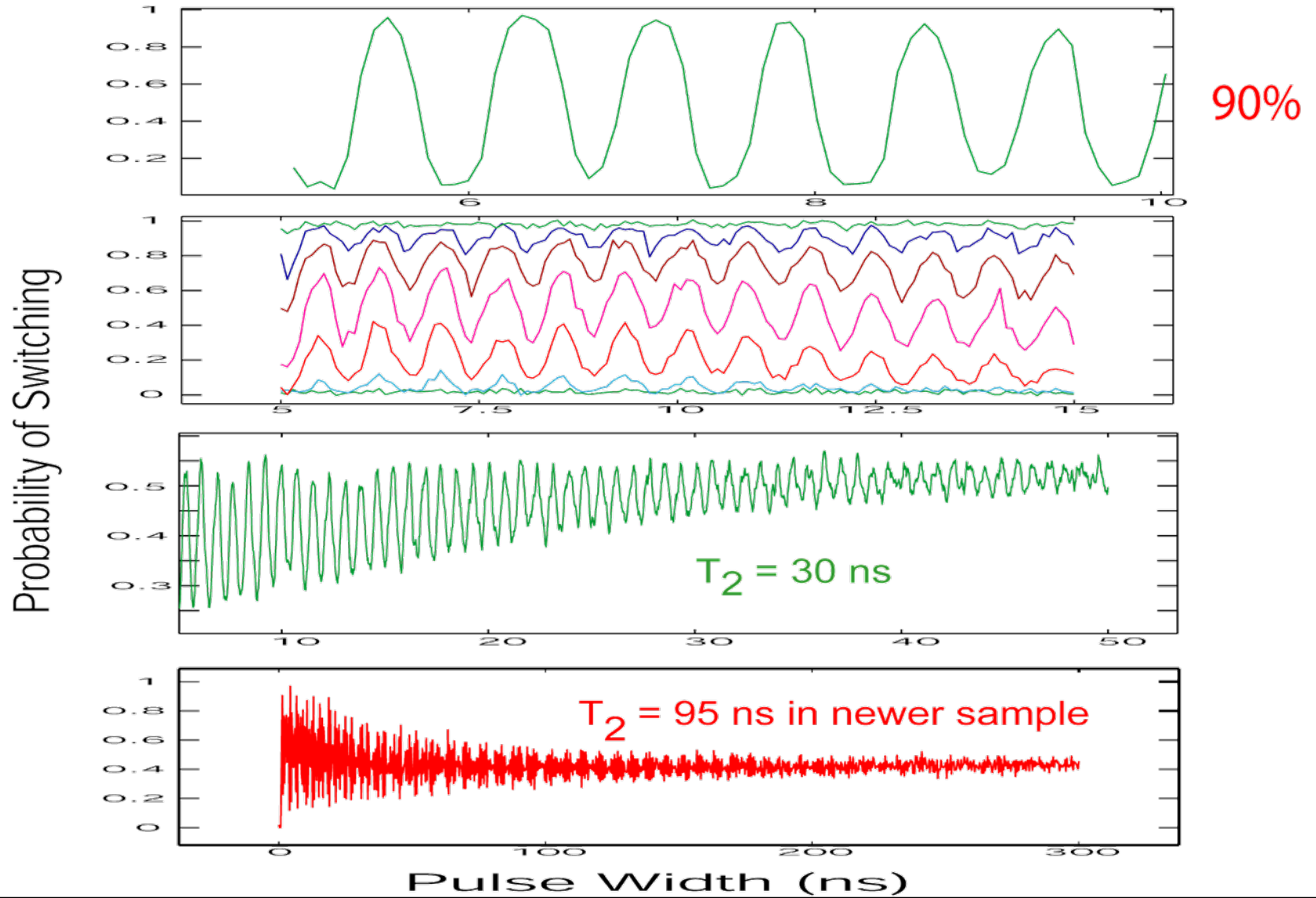


FIG. 20: The total relaxation, dephasing and decoherence times (T_1 , T_{ϕ} and T_2 , respectively) along the S line. We can see that T_{ϕ} (T_1) strongly increases (decreases) as a function of Φ_c . These facts cause there to be a window of desirable operating parameters for the qubit.

Experimental Demonstration of an Oscillator Stabilized Josephson Flux Qubit

R. H. Koch, G. A. Keefe, F. P. Milliken, J. R. Rozen, C. C. Tsuei, J. R. Kirtley, and D. P. DiVincenzo
IBM Watson Research Center, Yorktown Heights, New York 10598, USA



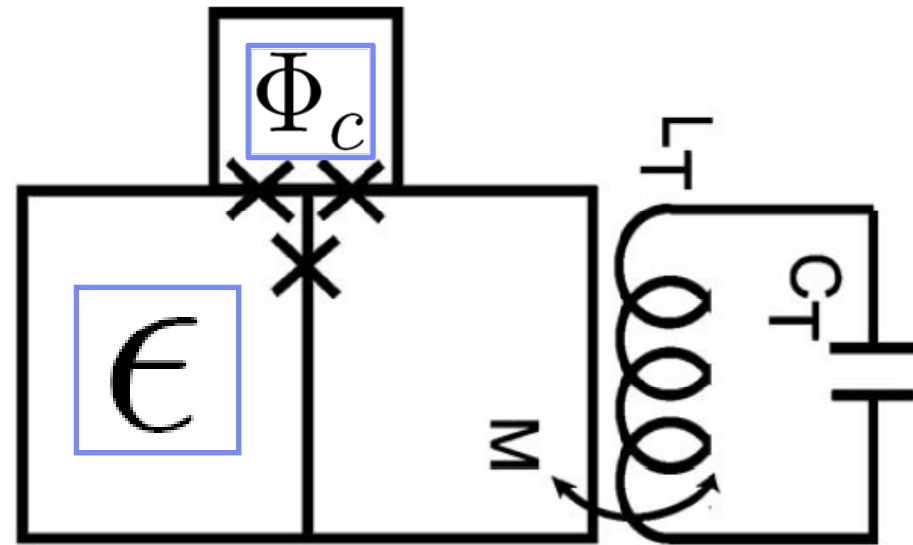
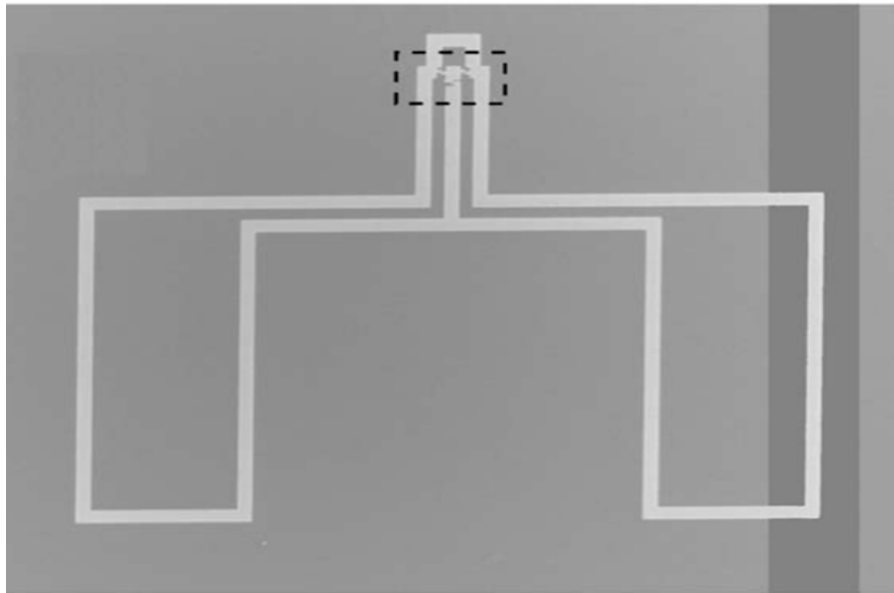
- IBM Qubit Koch *et al.* PRL **96**, 127001 '06; PRB **72**, 092512 '05.

■ Oscillator Stabilized Flux Qubit

- Three Josephson Junctions, Three loops
- High-Quality Superconducting Transmission Line

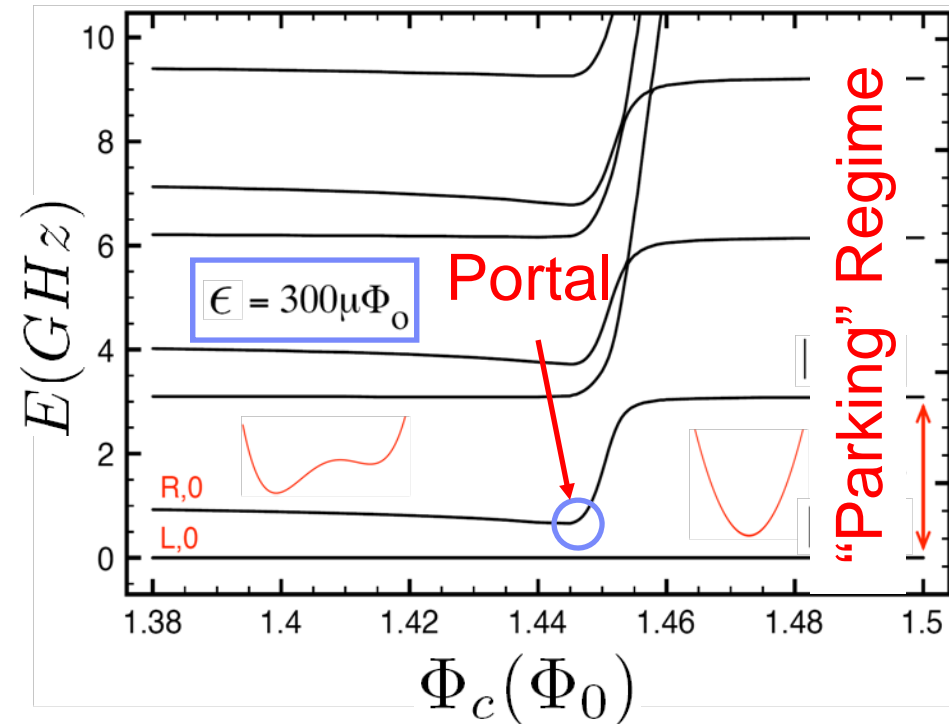
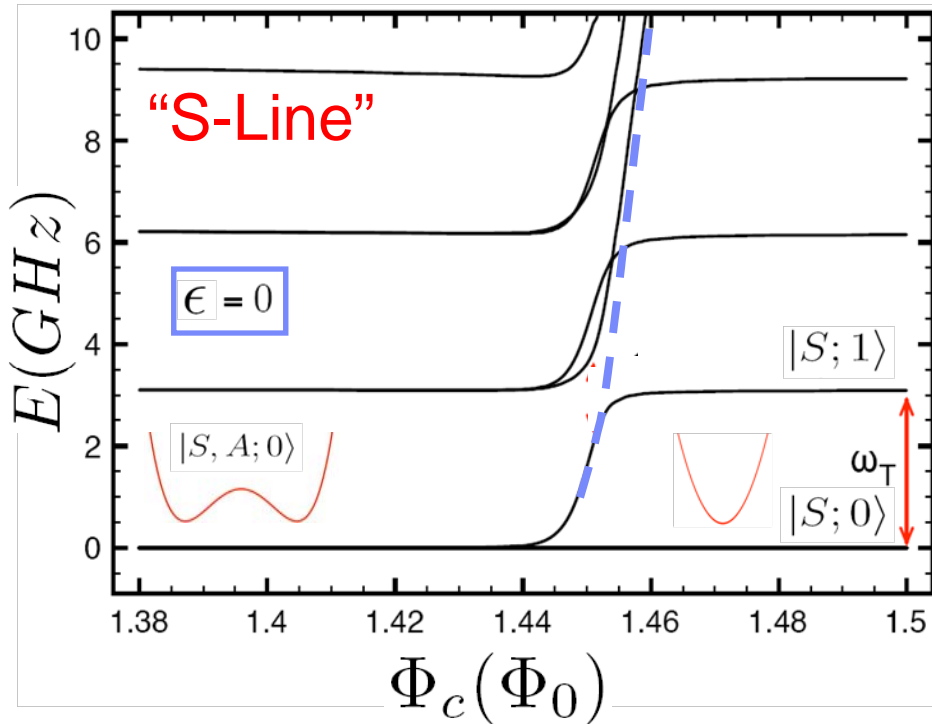
- $T_2 = 2.7\mu\text{s}$ (memory point); $T_1 = \sim 10\text{ns}$ (measurement point)

- Low-bandwidth operations

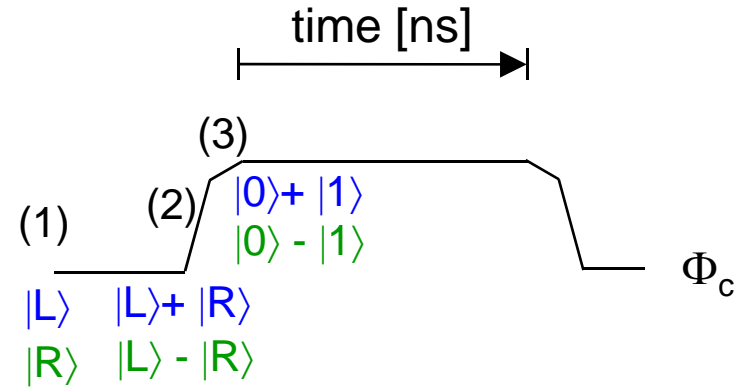
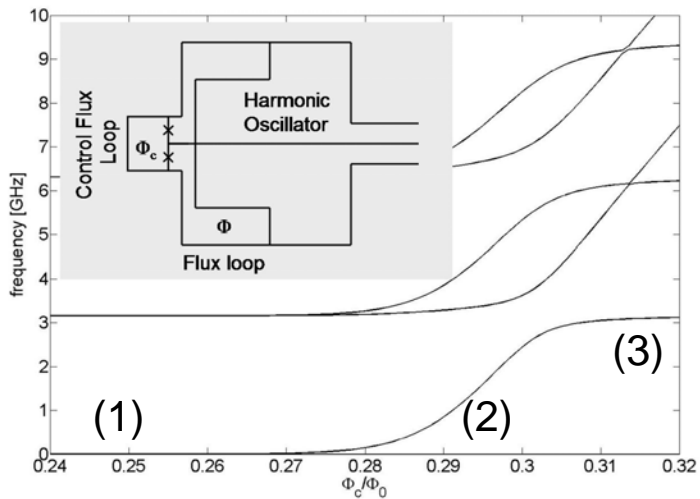


- Level Dynamics

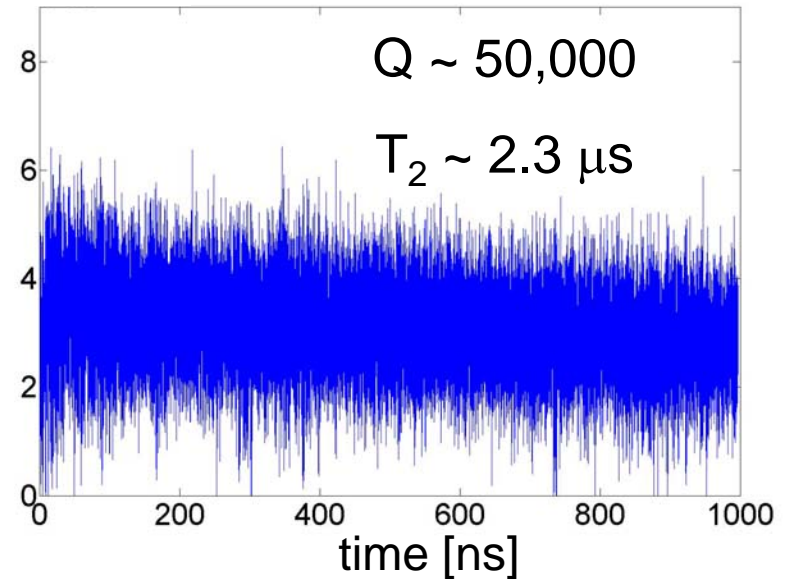
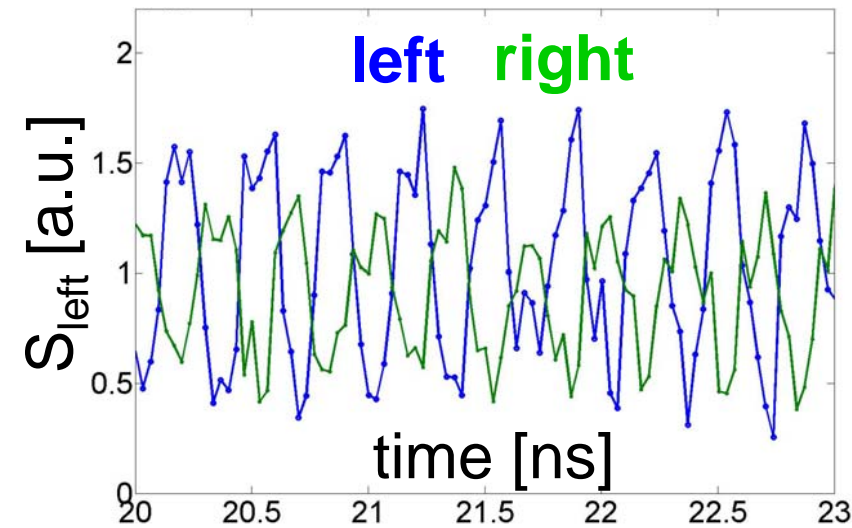
$$H = -\frac{1}{2}\Delta(\Phi_c)\hat{\sigma}_x + \frac{1}{2}\epsilon b(\Phi_c)\hat{\sigma}_z + \hbar\omega_T\hat{a}^\dagger\hat{a} + g(\Phi_c)(\hat{a} + \hat{a}^\dagger)\hat{\sigma}_z$$



Follow-up Experiment, March 2007 (unpublished)



Should observe “Larmor precessions” which measure quality of harmonic oscillator



T_2 increased by 300x !!

- One-qubit Gates summary

Gaussian Probability Distribution

■ **0-1 measurement: Fidelity > 99.99%**

■ **+ - measurement: Fidelity ~ 99.8%**

■ **Z – Gate: Fidelity > 99.99%**

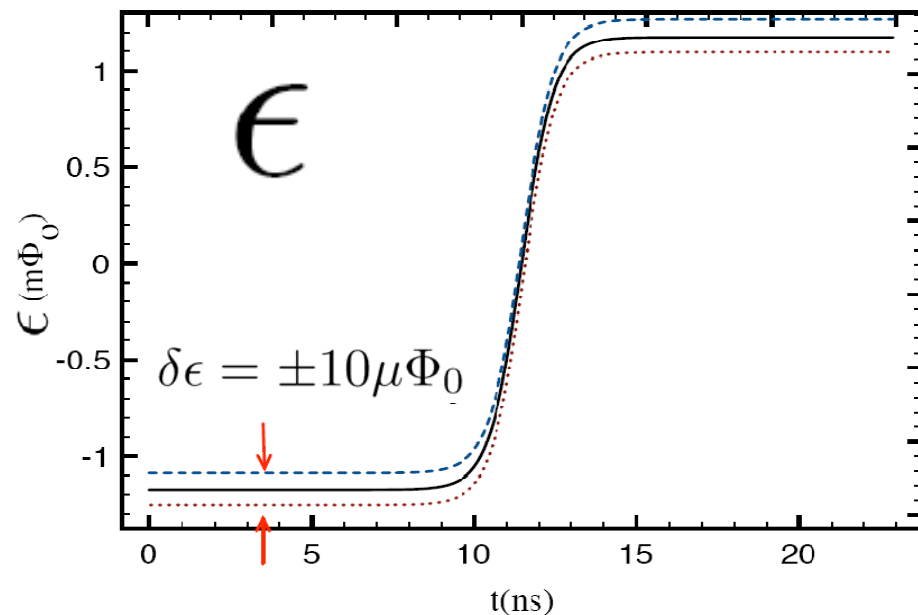
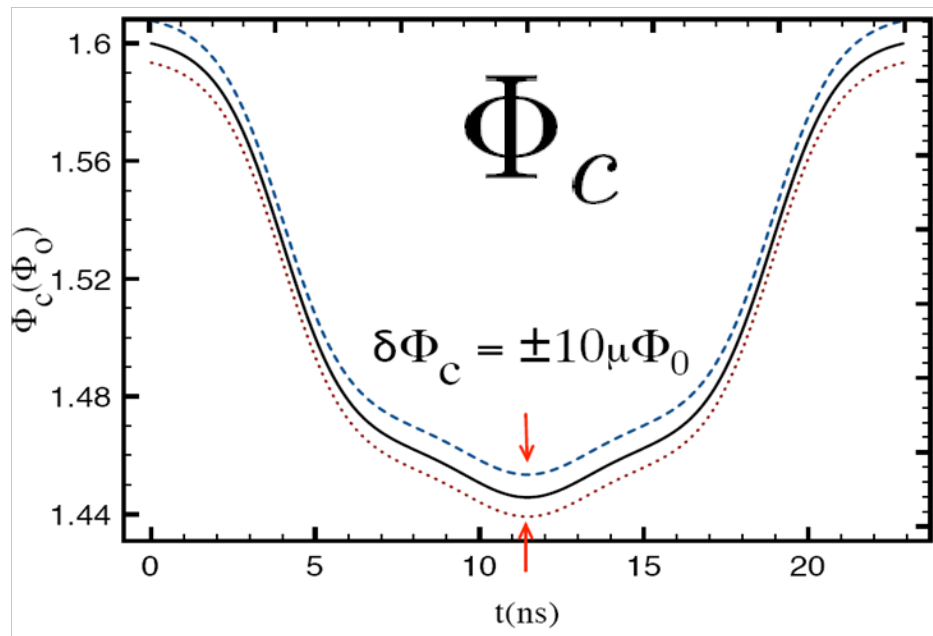
■ **Hadamard Gate: Fidelity ~ ~~98.7%~~**

~ 99.5%

■ **Memory Noise: 1% of error in $\sim 10^{-3}$ s**

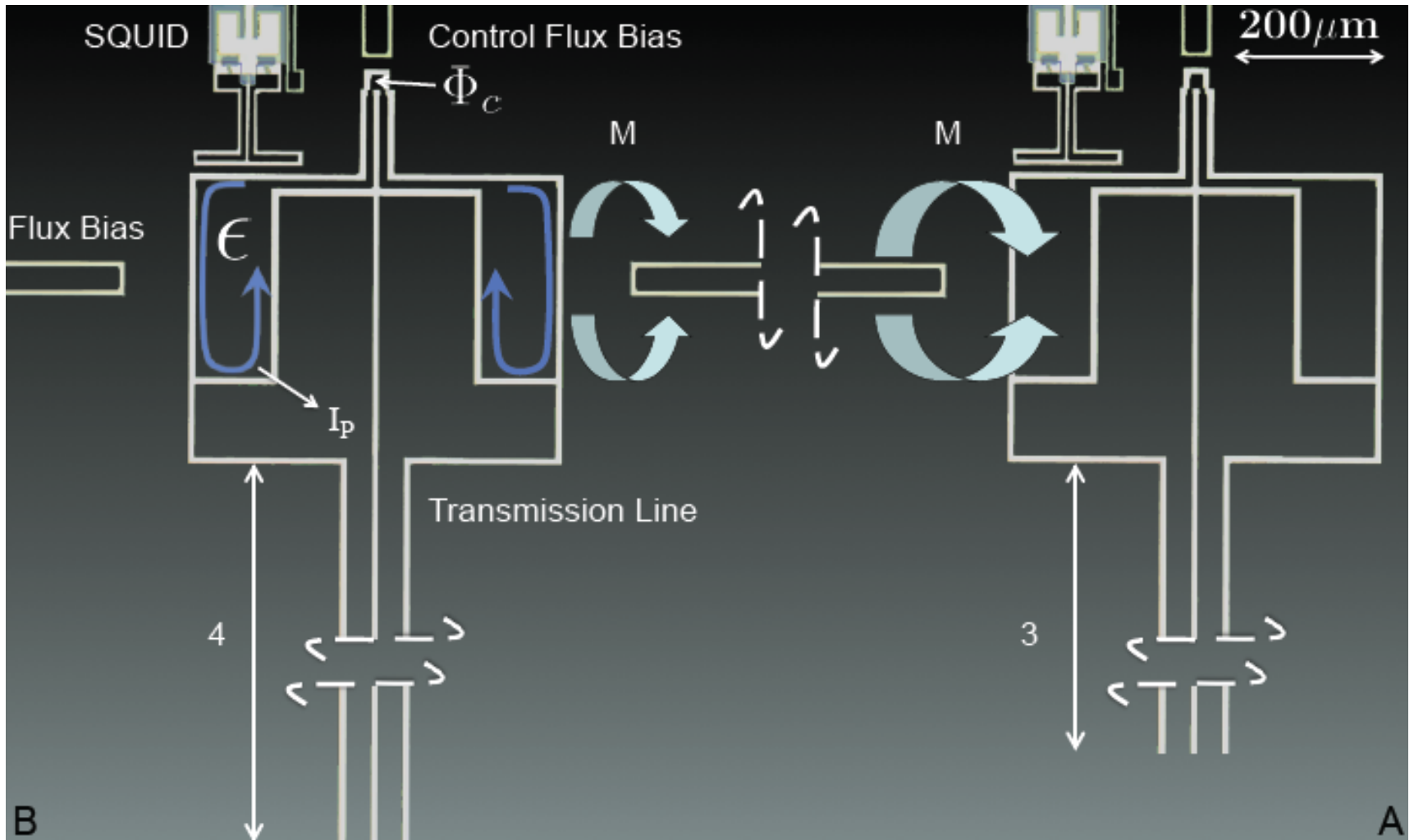
$$\frac{\delta\omega_{01}}{\delta\Phi_c} = \frac{1\text{Hz}}{10\mu\Phi_0}$$

- Low frequency noise:
 - 1/f flux noise (and other 1/f sources)
 - pulse jitter



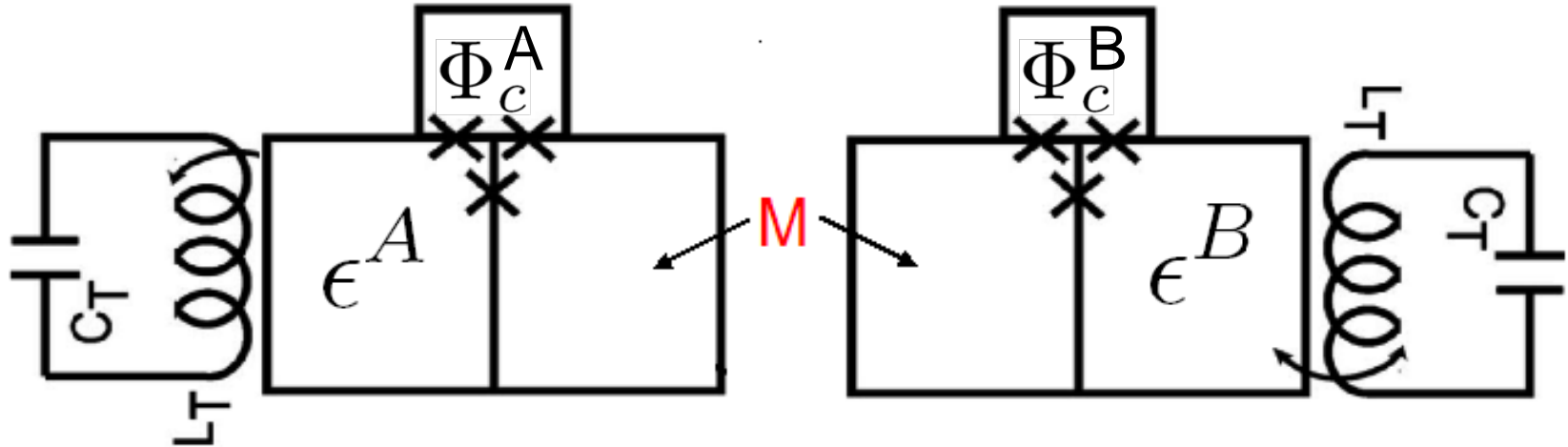
$$\delta t = 10ps, \quad \delta\Phi_c = 10\mu\Phi_0, \quad \delta\epsilon = 10\mu\Phi_0$$

Two qubit gate setup



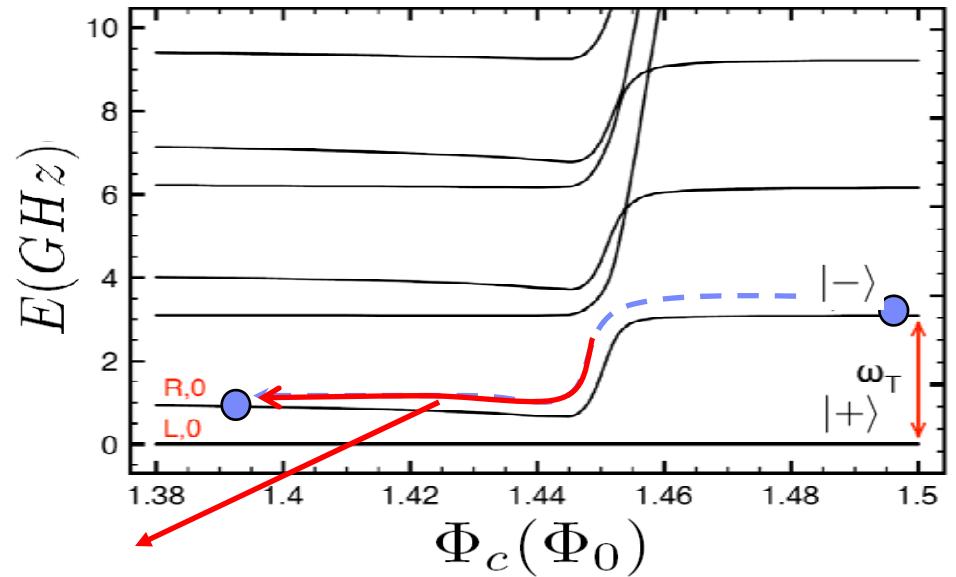
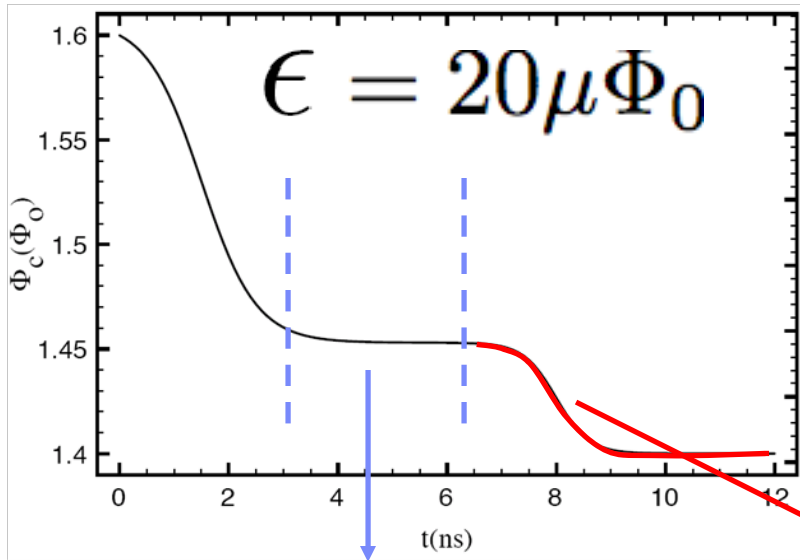
- Two-qubit Gate

Flux-Flux Coupling: **ZZ interaction**



$$H_I = J(\Phi_c^A, \Phi_c^B) \hat{\sigma}_z^A \otimes \hat{\sigma}_z^B$$

"|+>, |->" Measurement Gate



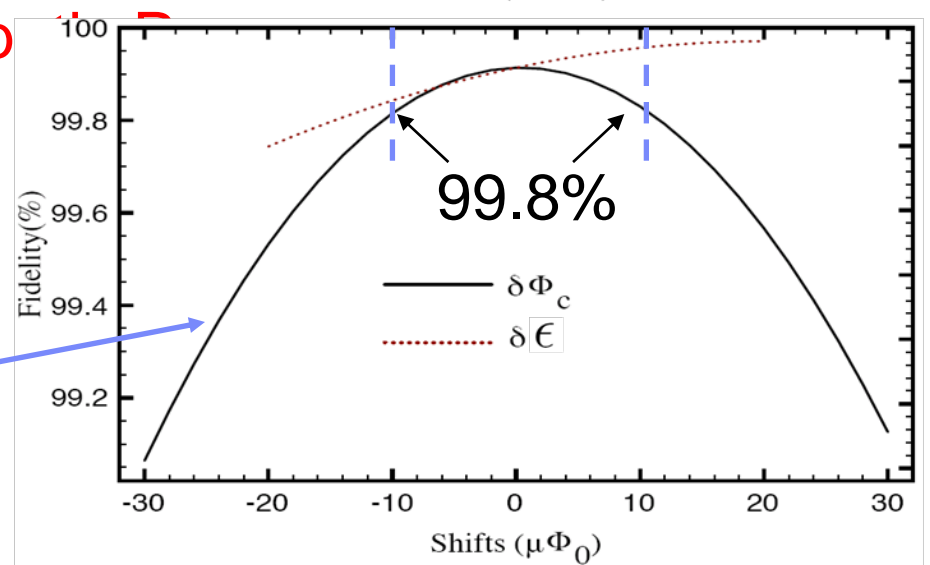
Non-Adiab

$$|\Psi_0\rangle = e^{-i\theta_0} \frac{1}{\sqrt{2}} (|0\rangle + |1\rangle)$$

$$|\Psi_1\rangle = e^{-i\theta_1} \frac{1}{\sqrt{2}} (|0\rangle - |1\rangle)$$

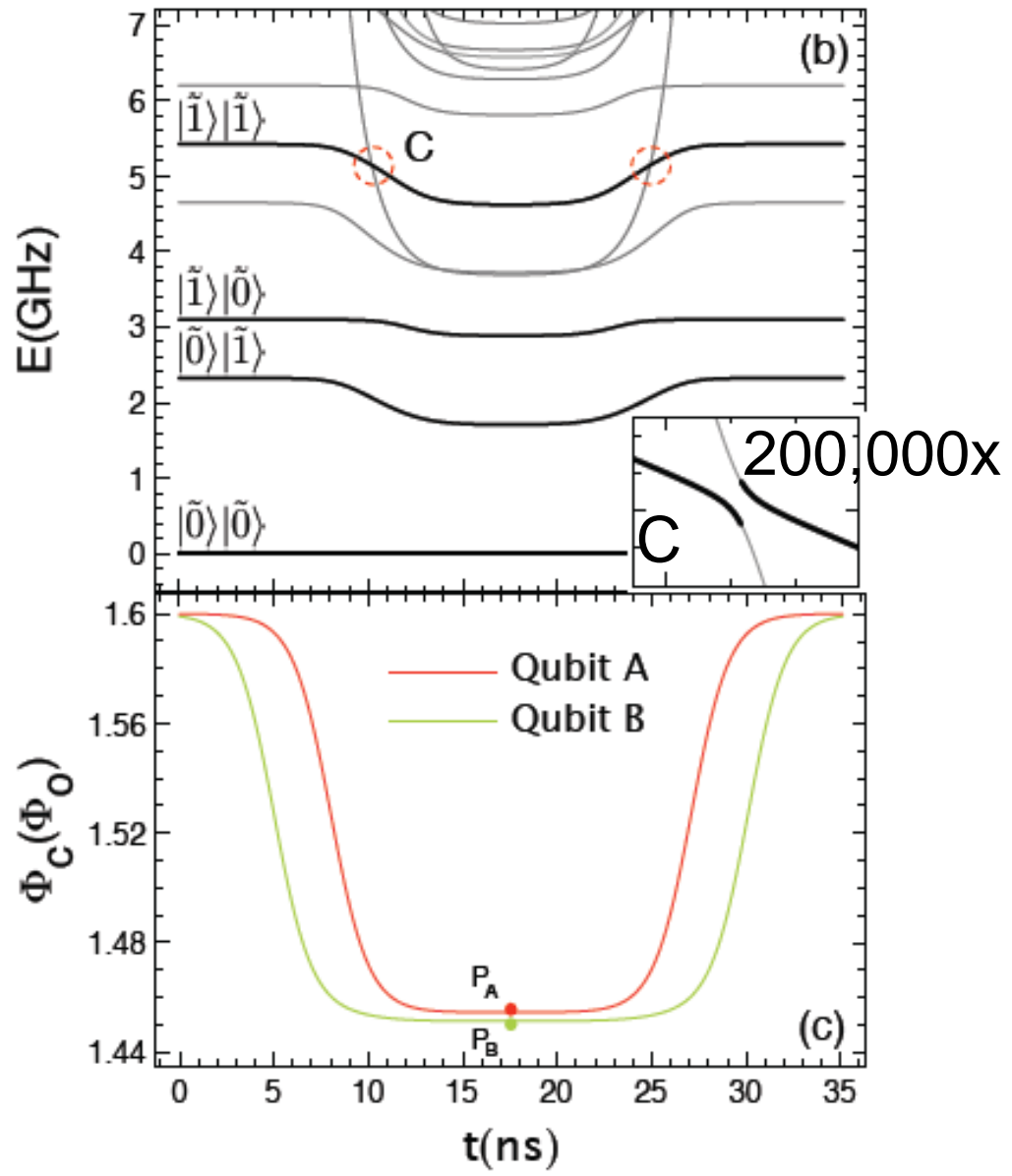
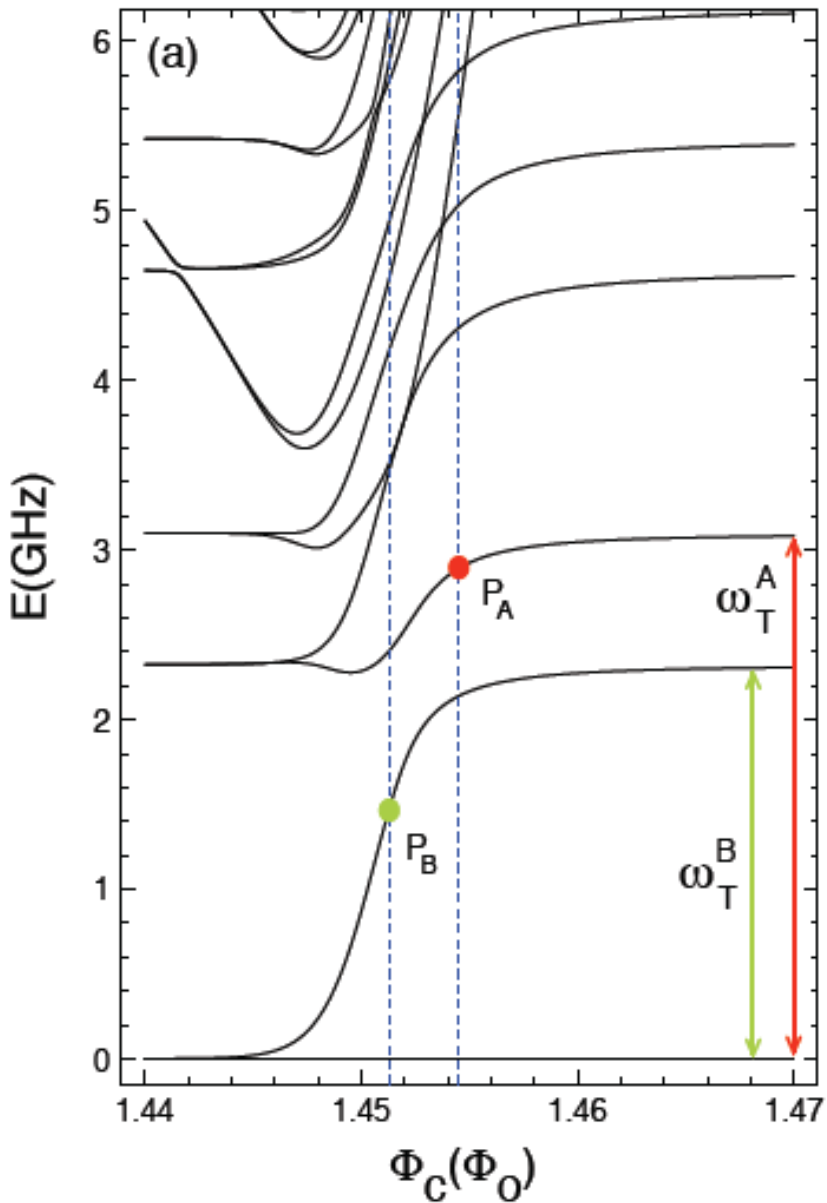
Leakage < 0.06%

Phase noise plays
the main role

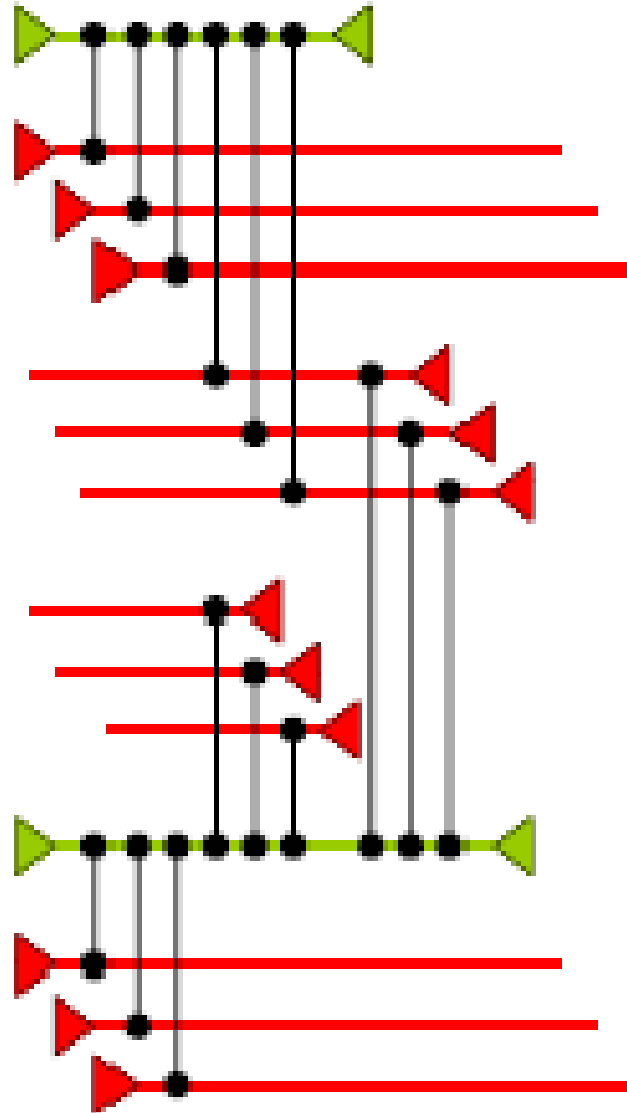
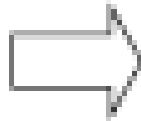
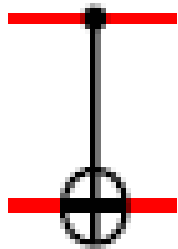


Two qubit gate: adiabatic controlled phase noise

almost completely Z type

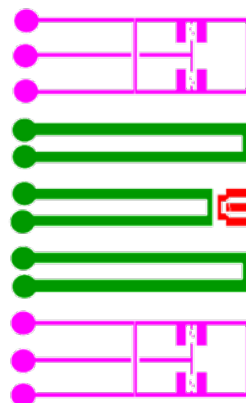


Logical CNOT

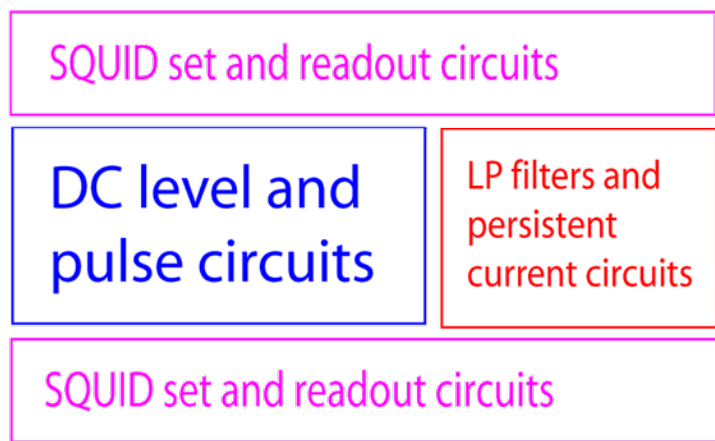
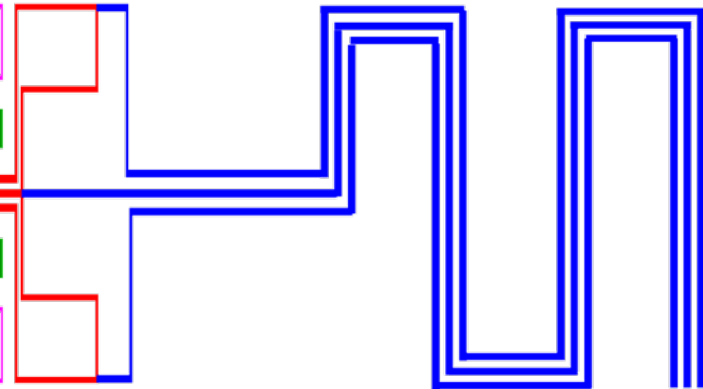


Some of the design and testing demos needed to build a 2-D array of qubits:

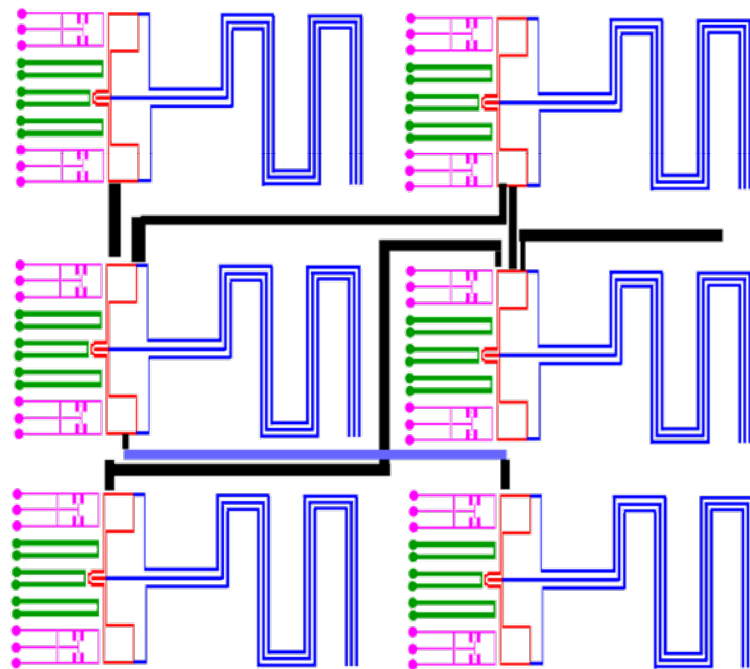
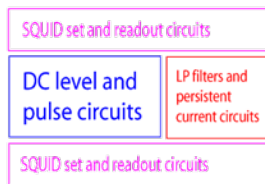
Use vias through the ground plane



Fold resonator to make it smaller



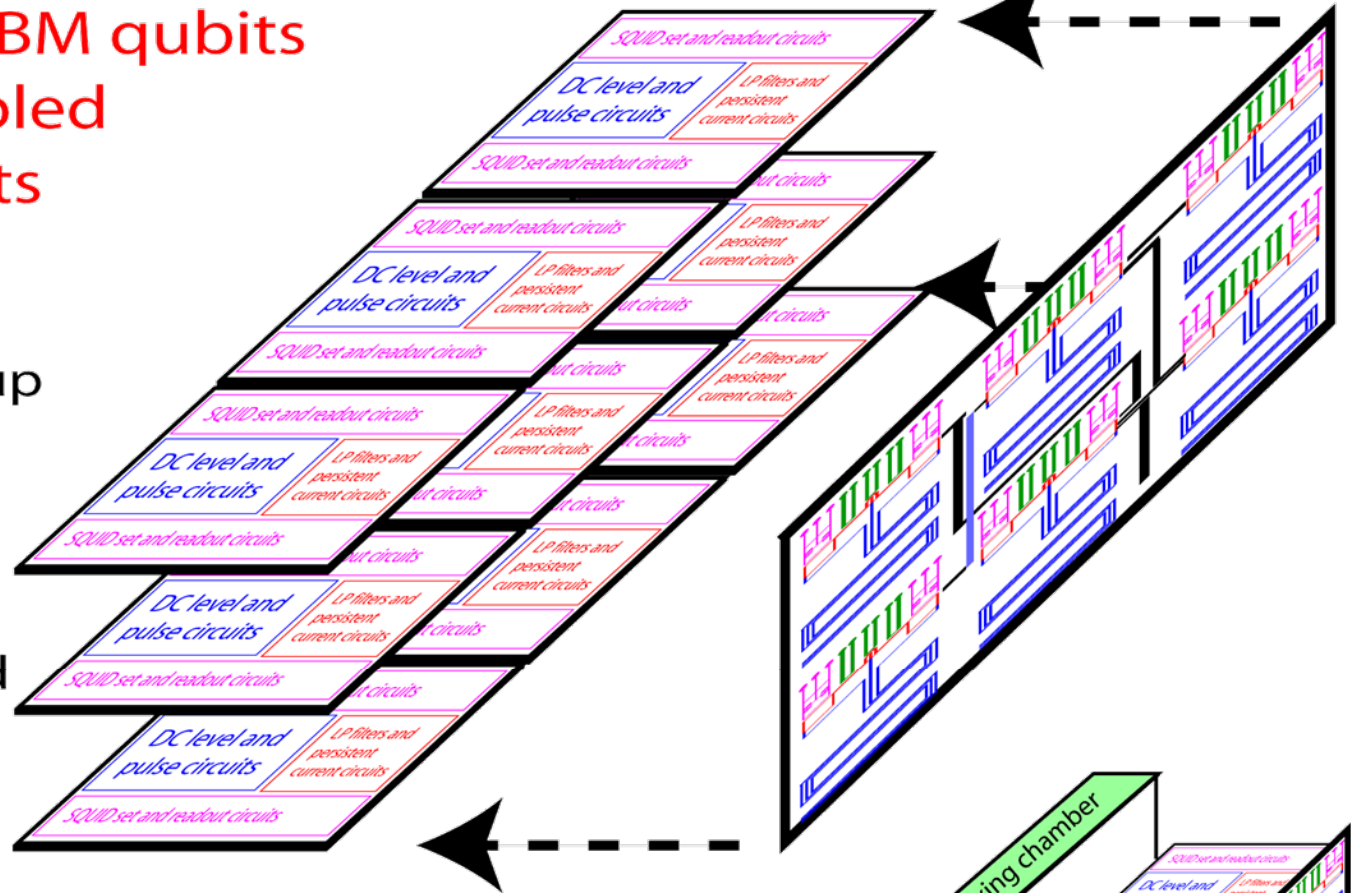
Make circuits smaller and make control circuit choices (CMOS vs SFQ and dc pulse vs microwaves)



Allow multiple qubit-to-qubit coupling, long range, and "coupling crossovers"

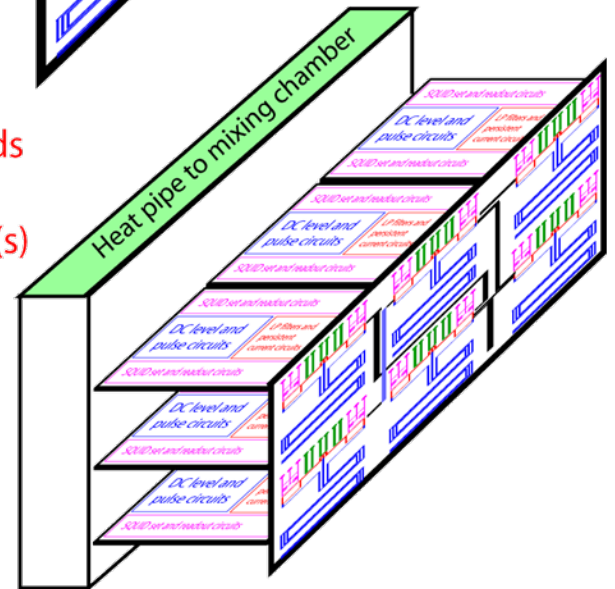
2-D array of IBM qubits to form Coupled Logical Qubits

IBM theory group has shown that a 2-d plane of qubits will have a much better threshold when compared to a 1-d or fractal design.



Use 3D Integration (3DI) methods to create dense array of qubits.
Superconducting ground plane(s) between qubits and circuits.
Superconducting bump bonds.

Following the ideas of [quant-ph/0604090](https://arxiv.org/abs/quant-ph/0604090)
"Noise Threshold for a Fault-Tolerant Two-Dimensional Lattice Architecture"
K. M. Svore, D. P. DiVincenzo, and B. M. Terhal



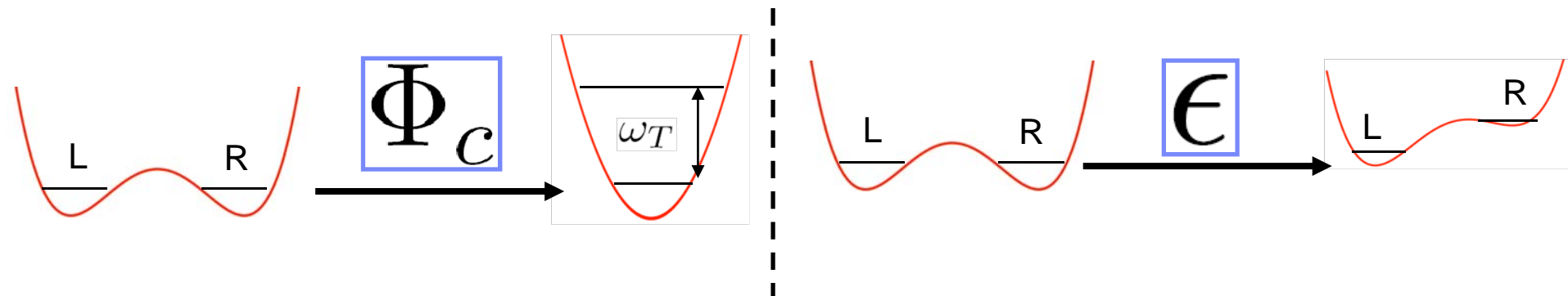
- Qubit Potential

Burkard, Koch, DiVincenzo PRB **69**, 064503 '04

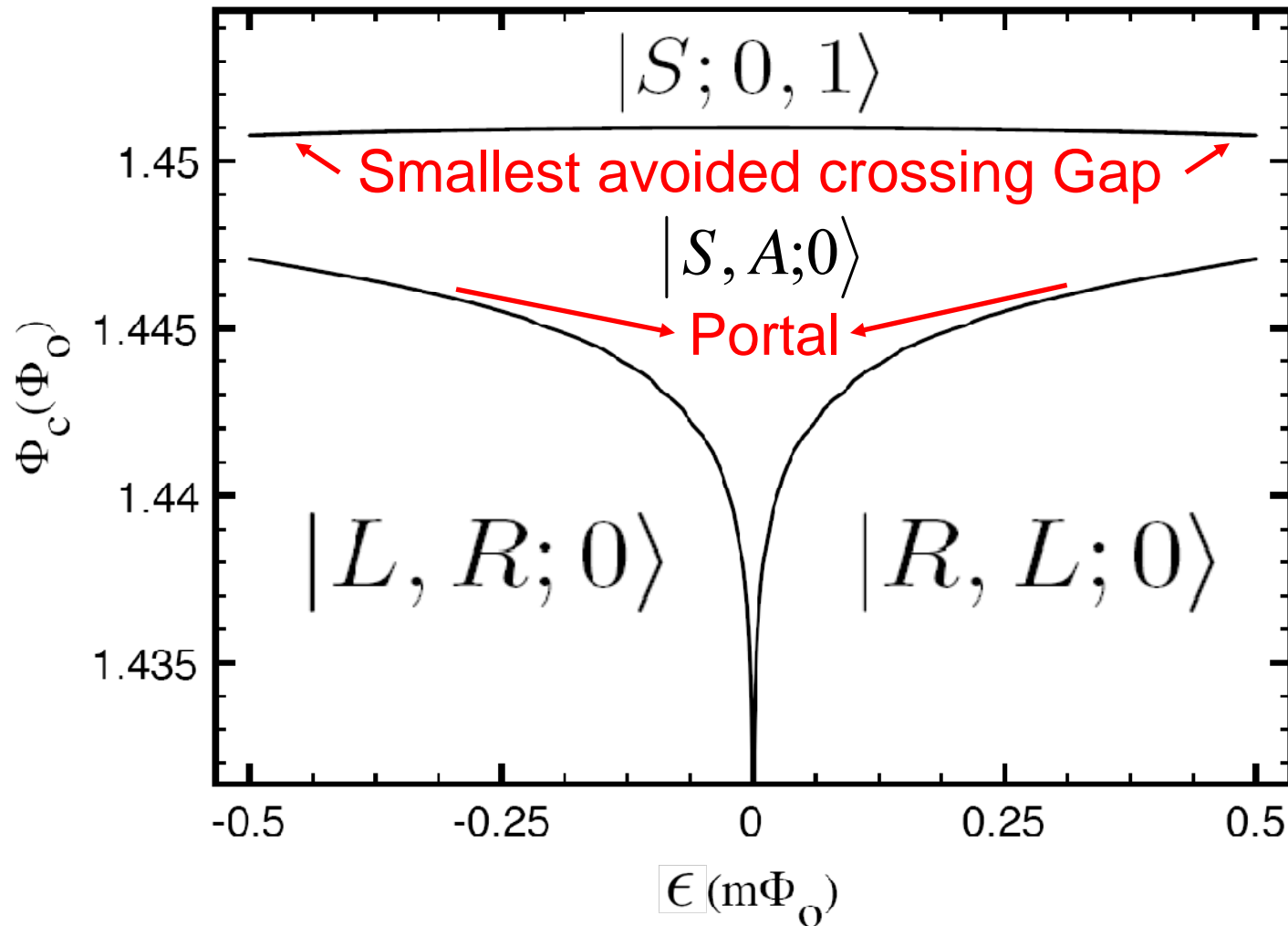
$$U(\varphi, t) = - \sum_i L_{J;i}^{-1} \cos \varphi_i + \frac{1}{2} \varphi^T \mathbf{M}_0 \varphi + \frac{2\pi}{\Phi_0} \varphi^T [(\bar{\mathbf{N}} * \Phi_x)(t) + (\bar{\mathbf{S}} * \mathbf{I}_B)(t)]$$

- Coupling qubit-Transmission Line

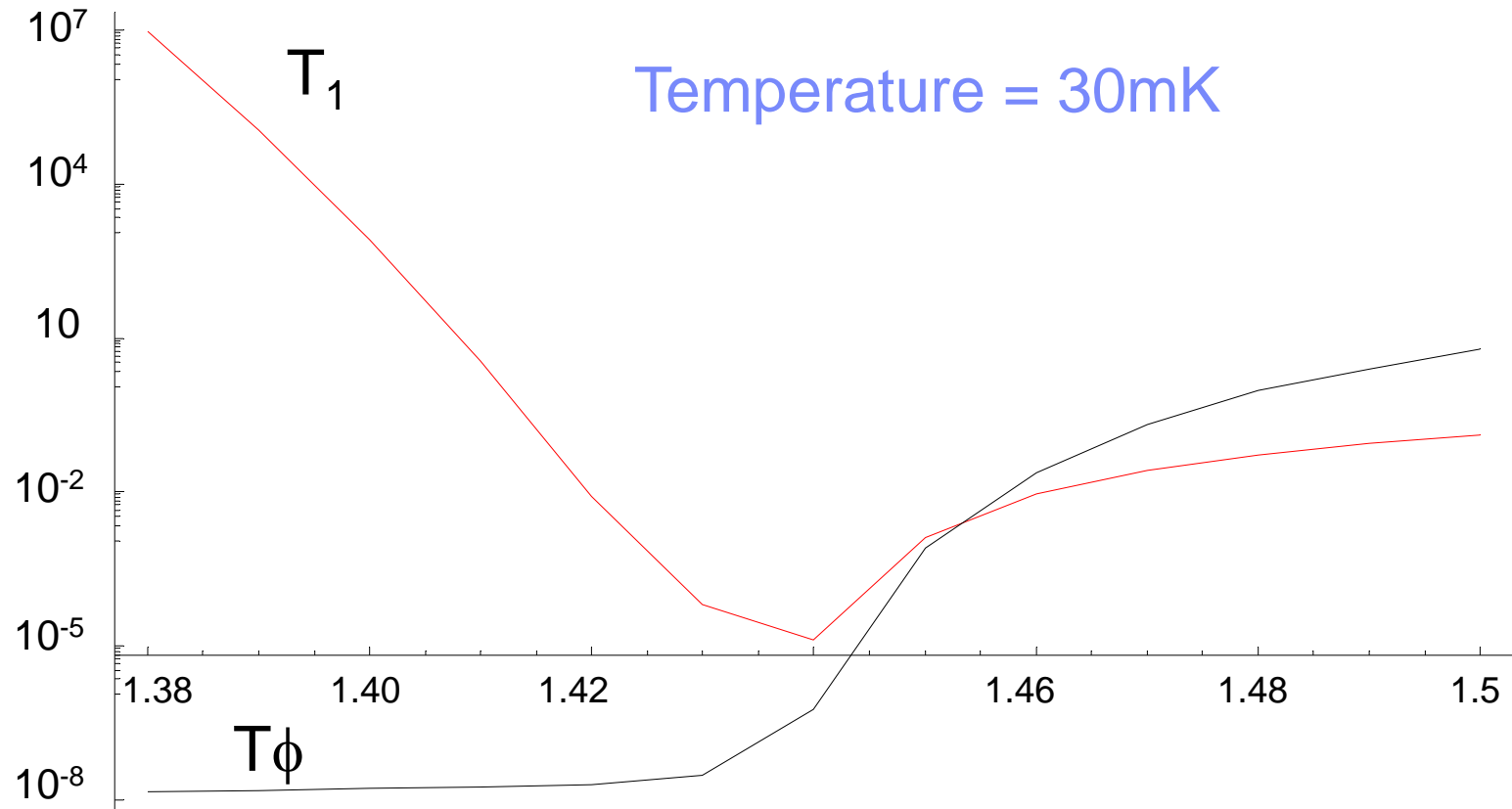
$$H = -\frac{1}{2} \Delta(\Phi_c) \hat{\sigma}_x + \frac{1}{2} \epsilon b(\Phi_c) \hat{\sigma}_z + \hbar \omega_T \hat{a}^\dagger \hat{a} + g(\Phi_c) (\hat{a} + \hat{a}^\dagger) \hat{\sigma}_z$$



- “Martini” Plot



Relaxation and Dephasing times (s)



- Band diagram

